Hydrothermal Synthesis and Characterization of TiO_2 for Photovoltaic devices

M.Malarkodi

(14PPH008)

Thesis submitted to

Avinashilingam Institute for Home Science and Higher Education for Women,

Coimbatore – 641 043.

In Partial Fulfilment of the Requirements for the

Degree of Master of Science in Physics

April, 2016.

Hydrothermal Synthesis and Characterization of TiO_2 for Photovoltaic devices

M.Malarkodi

(14PPH008)

Thesis submitted to

Avinashilingam Institute for Home Science and Higher Education for Women,

Coimbatore – 641 043.

In Partial Fulfilment of the Requirements for the

Degree of Master of Science in Physics

April,2016.

29/4/16

Signature of the Head of the Department

29/4/16

Signature of the Supervisor

ACKNOWLEDGEMENT

ACKNOWLEDGEMENT

I owe my sincere thanks to **Lord Almighty** and **My Lovable Parents** without whom I would have been nothing and showering their generous blessings upon me in all endeavors.

I wish to express my profound sense of gratitude **Shri. Dr. P.R.Krishnakumar**, Chancellor, Avinashilingam Institute for Home Science and Higher Education for Women, Coimbatore, for providing the facilities to conduct this study.

I extend my thanks to **Hon.Col.Dr. (Tmt.) Premavathy Vijayan,** M.Sc., M.Ed., Dip. Spl.Edn., M.Phil., Ph.D., Vice Chancellor (i/c), Avinashilingam Institute for Home Science and Higher Education for Women, Coimbatore, for providing flamboyant help towards the completion of the study.

I record my deep sense of gratitude and indebtedness to, **Dr. (Tmt.) A.Venmathi,** M.Sc, Dip.Ed, M.Phil, Ph.D. Registrar (i/c), Avinashilingam Institute for Home Science and Higher Education for Women, Coimbatore, for providing adequate help for the study.

I place on record my heartfelt thanks to **Hon.Col.Dr. (Tmt.) Saroja Prabakaran,** M.A.,Dip.Ed.,Ph.D.,Former Vice Chancellor, The Director, Hall of Residence, Avinashilingam Educational Trust Institutions Hostel, Coimbatore, for extending all possible help towards the completion of the study.

I gratefully record my sincere thanks to **Dr. (Tmt.) A. Parvathi**, M.Sc.,Dip. Ed., M.Phil., Ph.D., Dean, Faculty of Science, Avinashilingam Institute for Home Science and Higher Education for Women, Coimbatore, for timely help rendered throughout the course.

I whole heartily thank **Dr. (Tmt.) J. Shanthi,** M.Sc., M.Phil., Ph.D., Professor and Head of the Department of Physics, Avinashilingam Institute for Home Science and Higher Education for Women, Coimbatore, for her encouragement and generous help which was of great value.

I am very much indebted to my respectful guide **Dr. V. Sasirekha,** M.Sc., Ph.D., Assistant professor, Department of Physics, Avinashilingam Institute for Home Science and Higher Education for Women, Coimbatore, for her excellent, outstanding guidance, constructive criticism, motivation, valuable advice, untiring support, timely suggestions, constant encouragement and faster care rendered throughout course my investigation.

I sincerely thank all **the staff members** of the Department of Physics, Avinashilingam Institute for Home Science and Higher Education for Women, Coimbatore, for their help and support.

I would like to express my special thanks to **my parents**, **sister**, **my friends** and all **my well-wishers** for their constant encouragement, support and help in carrying out this work successfully.

MALARKODI.M

CONTENT

CONTENTS

LIST OF FIGURES

LIST OF TABLES

INTRODUCTION

CHAPTER - I

1. INTRODUCTION

The yearly increase in global energy consumption will result in the rise of demands towards natural resources such as coal, petroleum and natural gas. These natural resources will take thousands of years to form and it cannot be replaced as fast as they are being consumed. As a result, the reliability on the other sources of energy, which is renewable, will also rise [1]. But the need of energy increases day by day, due to this we look for another source in renewable energy. Renewable resources are natural resources that can be replenished in a short period of time. Solar power is promising, renewable energy resource that can be turned into electricity. Energy resource can be mainly classified into non-renewable energy and renewable energy.

1.1. NON RENEWABLE ENERGY SOURCES:

Nonrenewable source of energy includes fossil fuels such as coal, oil, petroleum, natural gas and also certain aquifers etc. these nonrenewable sources of energy are obtained naturally on our earth. But due to high energy needs and also the occurrence of reduction in these non-renewable energy sources from the earth region, most of the fossil fuels have been depleted and this led to certain natural disasters which are caused because of over usage of these sources [2-3].

1.2. RENEWABLE ENERGY SOURCES:

Renewable energy is generally defined as energy that comes from the natural resources such as sunlight, wind, ocean, tides, waves, geothermal etc. about 19% of global energy consumption comes renewable resources, accounted for an estimated 4.1% of total final energy use. For the past two decades hydropower made up about 3.7% and also an estimate of 1.9% was provided by power from wind, solar, geothermal and biomass and by biofuels.

Total worldwide renewable power capacity exceeded 1470 GW which is an increase of about 8.5% for the last two decades. And for the hydropower and PV solar power the raise is about 26% approximately [4].

Renewable enrgy technologies are suited for both rural and remote areas. A small area location is sufficient for construction these technologies. While many renewable energy projects are of large scale.

Most of the renewable enrgy sources derive their energy from the sun, either directly or indirectly. In addition to that hydro and wind are expected to be capable of supplying energy for the future generation almost for another one billion years.

1.3. PHOTOVOLTAIC DEVICE:

Solar cells are one type of photovoltaic cells which use a method of generating electrical power by converting energy of light into direct current electricity using semiconductors that exhibit the photovoltaic effect. The photovoltaic effect, electrons are transferred between different bands (usually from the valence bands to conduction bands) with in the material, resulting in the buildup of voltage between two electrodes. Photovoltaic is one of the fastest growing renewable energy technologies [5]. The electricity produced through solar technology is being widely used to power homes, cars and other appliances [6]. The complete structure of solar cells consists of a semiconductor, p-n junction photodiodes with a large light-sensitive area.

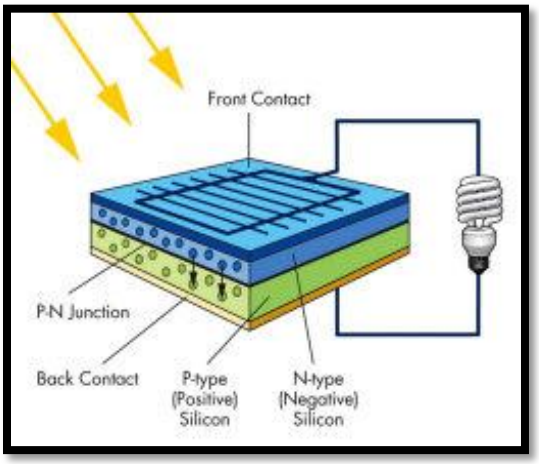

FIG 1.1, PHOTO VOLTAIC CELL

1.3.1 BENEFITS OF PV:

- Solar power is a renewable resource that is available everywhere in the world.
- Solar PV technologies are small and highly modular and can be used virtually anywhere, unlike many other electricity generation technologies.
- Unlike conventional power plants using coal, nuclear, oil and gas; solar PV has no fuel costs and relatively low operation and maintenance costs.

1.4. GENERATION OF SOLAR CELL:

Solar cell technologies are usually classified into three generations.

FIRST GENERATION SOLAR CELL:

- Single crystalline silicon (c-Si)

SECOND GENERATION SOLAR CELL:

- Amorphous silicon (a-Si)
- Cadmium-Telluride silicon (CdTe)
- Polycrystalline silicon (poly-Si)
- Copper-Indium-Gallium-Dieseline silicon (CIGS)

THIRD GENERATION SOLAR CELL:

- Dye sensitized solar cell (DSSC)
- Nanocrystal solar cells
- Photo electrochemical (PEC) cells
- Polymer solar cells

1.4.1. FIRST GENERATION SOLAR CELL:

First generation cells consist of large area, high quality and single junction devices. First generation technologies involve high energy and labour inputs which prevent any significant progress in reducing production costs. Single junction silicon devices are approaching the theoretical limiting efficiency of 33% and combined with high production costs are unlikely to achieve cost parity with fossil fuel energy generation.

ADVANTAGES:

- Broad spectral absorption range.
- High carrier mobilities.

DISADVANTAGES:

- Requires expensive manufacturing technologies.
- Growing and sawing of ingots is a highly energy intensive process.

1.4.2. SECOND GENERATION SOLAR CELL:

Second generation solar cells are usually thin film solar cells because when compared to crystalline silicon based cells they are made from layers of semiconductor materials only a few micrometers thick. The combination of using less material and lower cost manufacturing processes allow the manufacturers of solar panels made from this type of technology to produce and sell panels at a much lower cost.

ADVANTAGES:

- Lower manufacturing costs.
- Lower cost per watt can be achieved.
- Reduced mass.

DISADVANTAGES:

- Typically, the efficiency of thin-film solar cells are lower compared with silicon solar cells.
- Amorphous silicon is not stable.
- Increased toxicity.

1.4.3. THIRD GENERATION SOLAR CELL:

Third generation PV technologies are at the pre-commercial stage and vary from technologies under demonstration. It is aim to enhance poor electrical performance of second generation thin film technologies while maintaining very low production costs. Current research is targeting conversion efficiency of 30-60% while retaining low cost materials and manufacturing techniques.

1.5. DYE-SENSITIZED SOLAR CELL:

A Dye Sensitized Solar cell is a low cost solar cell belonging to the group of thin film solar cells. DSSC is one energy source in the photo-electrochemical cell family. DSSC is a solar cell using wide band gap semiconductor and sensitizer loading to absorb light, then, converting the light energy into electricity. Comparing to the silicon based solar cell, DSSC manufacturing process is easier and less expensive. The dye sensitize solar was first applied for solar cell in 1970's, but the efficiency was only 0.1% [7]. In 1991, Michael Gratzel described a DSSC with nano-crystalline $Tio_{2,}$ which had a 15 nm average size, for the anode material, and a ruthenium complex sensitizer with high turnover number, achieving a 7% efficiency [8].

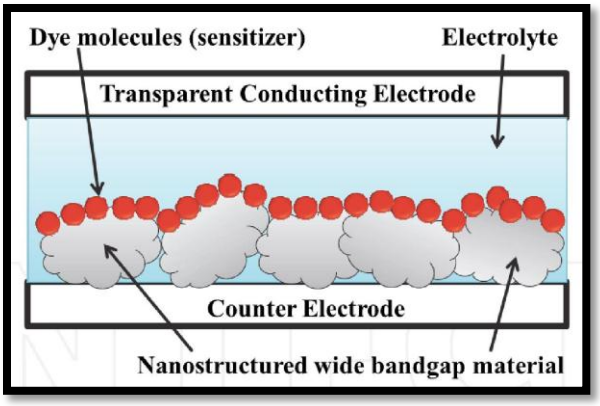

FIG 1.2, SCHEMATIC STRUCTURE OF THE DSSC

1.6. DSSC OPERATING PRINCIPLE:

Photo-excitation of the sensitizer is followed by electron injection into the conduction band of the mesoporous oxide semiconductor. The dye molecule is regenerated by the redox system, which itself is regenerated at the counter electrode by electrons passed through the load. Potentials are referred to the normal hydrogen electrode. The open-circuit voltage of the solar cell corresponds to the difference between the redox potential of the mediator and the Fermi level of the nanocrystalline film indicated with a dashed line.

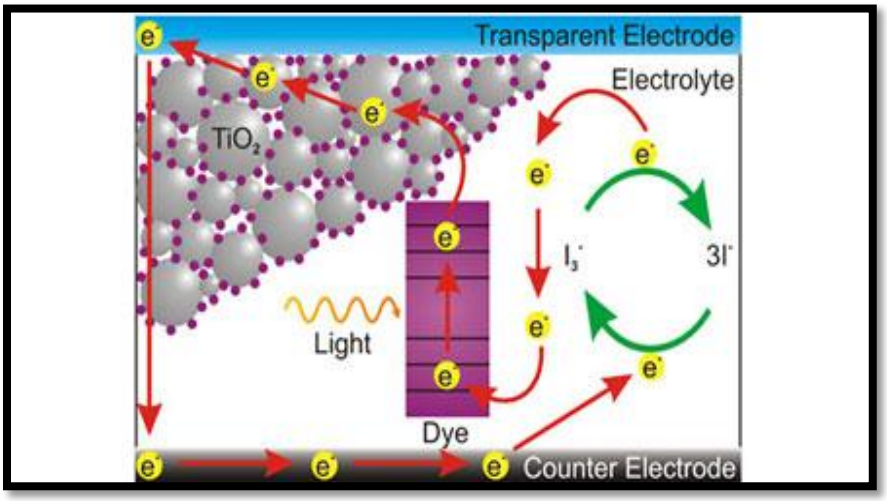

FIG 1.3, OPERATION PRINCIPLE OF DSSC

1.7. DSSC WORKING PRINCIPLE:

Dye-sensitized solar cells are photo electrochemical device where several electron transfer processes run in parallel and in competition. In a DSSC optical absorption and charge generation are separate functions. DSSCs are photo regenerative device [9].

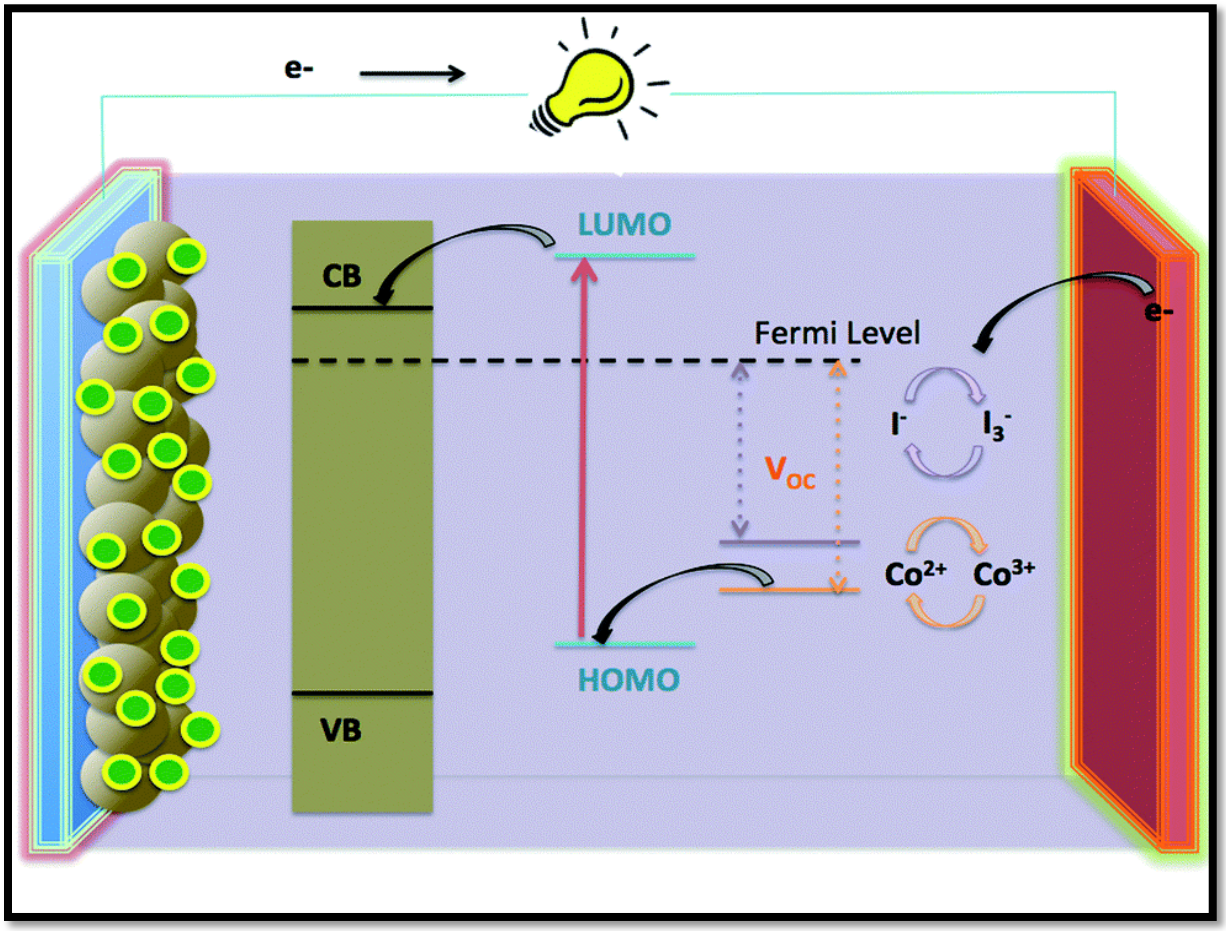

FIG 1.4, SCHEMATIC DIAGRAM OF WORKING PRINCIPLE OF DSSC

$$S + h\nu \longrightarrow S^* \qquad (1)$$

S: ground state of the dye,

S*: excited state of the dye

S^+: oxidized state of the dye.

$$S^* + Tio_2 \longrightarrow S^+ + e^-(Tio_2) \quad (2)$$

$$e^-(TiO_2) + \text{Electrode} \longrightarrow TiO_2 + e^-(\text{Electrode}) + \text{energy} \quad (3)$$

$$S^+ + e^- \longrightarrow S + I_3^- \quad (4)$$

$$2e^-(\text{Electrode}) + I_3^- \longrightarrow 3I^- + \text{Electrode} \quad (5)$$

Nano crystalline TiO_2 was deposited on the conducting electrode to provide the necessary large surface area where dye molecules get absorbed. The absorption of dye molecules get excited from the highest occupied molecular orbitals (HOMO) to the lowest unoccupied molecular orbitals (LUMO) state as presented in equation (1).

Once an electron injected into the conduction band of the wide band gap semiconductor nanostructured TiO_2 film, the dye molecule (photosensitizer) become oxidized, equation (2). The injected electron is transported between the TiO_2 nanoparticles and then gets extracted to a load where the work done is delivered an electric energy, equation (3). To mediate electron between the TiO_2 photo electrode and the carbon coated counter electrode electrolyte containing I^-/I_3^- redox ions is used to fill the cell. The oxidized dye molecules are regenerated by receiving electrons from I^- ion redox mediator that will oxidized to I_3^-, equation (4). The I_3^- substitutes the donated electron internally with that from the external load and gets reduced back to I^- ion, equation (5).

Upon illumination, photo excitation of the dye results in the injection of an electron into the conduction band of the oxide. The oxidized sensitizer thus formed can recombine with the injected electron or it can be regenerated by the electron donor in the electrolyte. Also relaxation of the excited dye before electron injection may occur. The photo generated electron travels through the mesoporous oxide film by a random walk process towards the external contact [10]. The extracted electron can then perform work in an external circuit and return to the counter electrode. The oxidized species in the electrolyte produced upon the dye regeneration step diffuses to the platinum coated counter electrode, where it is reduced back, closing the regenerative cycle. The major loss

channel in the process is the recombination of the injected electrons with the oxidized redox mediator. The timescale of the different processes is the key point for obtaining high energy conversion efficiency of these devices.

The maximum theoretical value for the photo voltage at open circuit condition was determined by the potential difference between the conduction band edge of the TiO_2 and the redox potential of the I^-/I_3^- couple in the electrolyte. Dye-sensitized solar cells are highly complex systems. There are a lot of processes interconnected with each other and the chemical complexity of the device makes it difficult to study separately the single processes affecting the functioning of the cell [11].

1.7.1. ADVANTAGES OF DSSC:

- DSSC use low cost materials, are simple to manufacture, and are technically attractive.
- DSSCs can be replacements for existing technologies in "low density" applications like rooftop solar collector, where mechanical reliability and light weight of the glass-less collector are important factors.
- The process of injecting an electron directly into the TiO_2 is qualitatively different to that occurring in a traditional cell, where the electron is "promoted" within the original crystal. In theory, given low rates of production, the high energy electron in the silicon could re-combine with its own hole and generates less volume of current.
- A result of these "differential kinetics", DSSCs work even in low-light conditions, allowing them to work under cloudy skies and non-direct sunlight when traditional designs would suffer a "cutout" at some lower limit of illumination, when charge carrier mobility is low and recombination becomes a major issue. The cutoff is so low that this technology is being considered for indoor use, collecting energy for small devices from the light in the house.
- Common semiconductor systems suffer noticeable decrease in efficiency as the cells heat up internally. DSSCs are normally built with only a thin layer of conductive plastic on the front layer, allowing them to radiate away heat much easier, and therefore operate at lower internal temperatures.

- The dye sensitized solar cell is a brilliant idea because it applies different mechanisms and has many advantages compare with traditional semiconductor solar cell. The DSSC technology will be an important renewable energy source in future. It may be possible to use mixed dye to overcome the band absorption limits of each dye to improve the overall efficiency.

1.7.2 DISADVANTAGES OF DSSC:

- Current efficiency is still relatively low compare with traditional semiconductor solar cells.
- Dyes will degrade when exposed to ultraviolet radiation that limits the lifetime and stability of the cells a barrier layer will increase the cost and may lower the efficiency.
- Generally, DSSC technology uses liquid electrolyte that has temperature stability problems. At low temperatures, the electrolyte can freeze, stopping power production and potentially leading to physical damage.
- The electrolyte solution contains volatile organic solvents permeate plastics, precludes large-scale outdoor application and flexible structures.
- Although the dye is highly efficient at converting absorbed photons into free electrons in the TiO_2, only photons absorbed by the dye will produce electric current. The rate of photon absorption depends on the absorption spectrum of the sensitized TiO_2 layer and upon the solar flux spectrum. The overlap between these two spectra determines the maximum possible photocurrent.
- DSSC technology may not attractive for large-scale deployments where higher-efficiency cells are more viable, although more expensive. But, even small increase in the DSSC conversion efficiency may make them suitable for some of these roles [12-13].

1.8. TITANIUM DIOXIDE (TiO_2):

Titanium dioxide, also known as titanium (IV) oxide or titania, is a naturally occurring oxide of titanium and its chemical formula is TiO_2 [14-16]. The three most

studied crystalline modifications of titania are Anatase, Rutile and Brookite. Rutile phase is most stable as compared to anatase and brookite phase. At low temperature it shows anatase phase and after heating treatment it in converted to rutile phase. TiO_2 is widely used as a pigment because of its high refractive index. Each crystalline structure specific exhibits specific physical properties such as band gap, surface states [17-18]. Anatase and rutile are well known photo catalysts with anatase generally showing much higher photo catalytic activity [19-20].

PHASE	CRYSTAL SYSTEM
Anatase	Tetragonal
Rutile	Tetragonal
Brookite	Orthorhombic

TABLE 1.1, CRYSTAL SYSTEM OF DIFFERENT PHASES OF TiO_2

1.8.1. CHARACTERISTICS OF TiO_2:

- TiO_2 is amphoteric in nature
- It is insoluble in water as acids
- It shows high room temperature resistivity, with specific resistivity of 9500 Ω
- It has a melting point of 1610°C and boiling point of 3000°C
- It shows temperature dependent paramagnetic susceptibility

1.8.2. APPLICATION OF TiO_2:

- TiO_2 is also an effective opacifier in powder form, where it is employed as a pigment to provide whiteness and opacity to products such as paints, coatings, plastics, papers, inks, foods, medicines as well as most toothpastes.
- In cosmetic and skin care products, titanium dioxide is used both as a pigment, sunscreen and a thickener because of its high refractive index (n=2.7), its strong

UV light absorbing capabilities and its resistance to discolouration under ultraviolet light.

- Used for Anti-fogging glasses, self-cleaning glass, anti-bacterial, anti-viral, fungicidal, anti-soiling, self-cleaning, deodorizing, air purification, water treatment water purification.
- Used in electronic components like capacitors [21].
- It has been extended to medical applications such as use in an artificial heart valve and in dental implants [22-23].

1.8.3. NEED OF TiO_2:

- As the size of the TiO_2 particles decreases, the fraction of the atoms located at the surface increases with higher surface area to volume ratios, which can further enhance the catalytic activity.
- The increase in the band gap energy with decreasing nanoparticle size can potentially enhance the redox potential of the valence band holes and the conduction band electrons, allowing photo-redox reactions, which might not otherwise proceed in bulk materials, to occur readily.
- By a decrease in particle size below a certain limit, surface recombination processes became dominant. Since most of the electrons and holes were generated close to the surface and surface recombination was faster than interfacial charge carrier transfer processes.

1.8.4. TiO_2 IN DYE SENSITIZED SOLAR CELL:

TiO_2 nanoparticles based dye-sensitized solar cells are a highly promising approach, giving efficiencies over 10%. The dye molecules are absorbed into the surface of sintered TiO_2 nanoparticles. The incident light is harvested by the dye, and an electron is injected into TiO_2 where it is transported through the TiO_2 nanoparticles to reach an electrode.

In dye sensitized solar cell TiO_2 nanoparticles are used as charge separators and conductors because of their unique ability of forming a huge network for the electrons to travel through. They are transparent nanoparticles. The dye molecules are absorbed on

the surface of the TiO_2 nanoparticles. When a light (photon) hit the dye molecule the electrons are generated.

The space in between the TiO_2 nanoparticles are filled with an electrolyte (iodide), which plays the role of transferring electrons from the cathode to the dye. This happens when a dye molecule releases an electron where it needs another one to replace it.

The transfer of electrons from the cathode of the dye-sensitized solar cell travels randomly from one TiO_2 nanoparticle to another particle until they reach the anode. The size and density of the TiO_2 nanoparticles can affect the journey of an electron. The defects in the nanoparticles results in electron lose to the iodide solution.

The optimized size and density of the TiO_2 nanoparticles play a major role in building a dye-sensitized solar cell. The most challenging task in building a dye-sensitized solar cell is creating a high surface area and also the allocation of maximum safe pathways for the flow of electron. When a photon of light strikes dye molecule, the energy from the photon is absorbed by the dye molecule and emits an electron by entering in to an excited state. The emitted electron travels through the TiO_2 nanoparticles until reaches the anode. If the defects exist in the TiO_2 nanoparticles then the electrons are lost in to the iodide solution.

When all these process are completed an electric current is generated. The fabrication of high efficiency dye-sensitized solar cell is based on the controlled structure and defects of TiO_2 particles.

1.9. ANATASE TiO_2:

Anatase is one of the three mineral forms of titanium dioxide, the other two being brookite and rutile. It is always found as small, isolated and sharply developed crystals. The TiO_2 anatase converts to rutile generally at the annealing of 600-700°C. some researchers have also found it to achieve rutile structure at 500°. Thus, anatase and rutile phase strongly depends on thermal treatment conditions. Anatase structure is tetragonal, with two TiO_2 formula unit (six atoms) per primitive cell. Lattice parameters

are, a=b=3.7710 Å and c=9.430 Å with c/a ratio of 2.5134 [24-25].

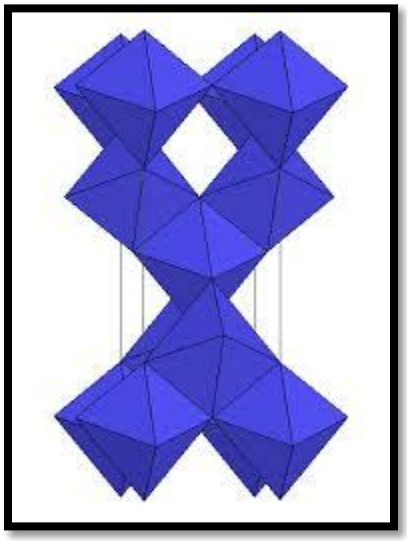

FIG 1.5, CRYSTAL STRUCTURE OF ANATASE

1.10. RUTILE TiO_2:

Rutile is a mineral composed primarily of titanium dioxide, TiO_2. Titanium dioxide has a stable phase rutile its unit cell contains Ti atoms occupying the center of a surrounding core composed of six oxygen atoms placed approximately at the corners of a quasi-regular octahedron. The lattice parameters are a = b = 4.5933 Å and c = 2.9592 Å with c/a ratio of 0.6442 [26-27].

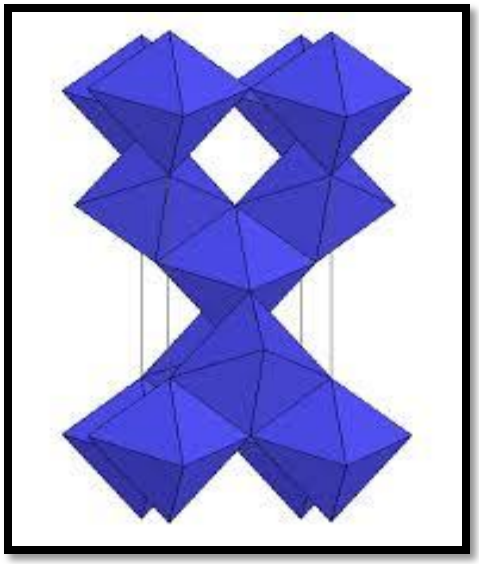

FIG 1.6, CRYSTAL STRUCTURE OF RUTILE

1.11. BROOKITE TiO_2:

Brookite is the orthorhombic variant of titanium dioxide, TiO_2. The brookite structure is more complicated and has a larger cell volume as compared to anatase and rutile. It is also the least dense of the least dense of the three forms. The unit cell is composed of eight formula units of TiO_2 and is formed by edge sharing TiO_2 octahedra, similar to rutile and anatase [28-31].

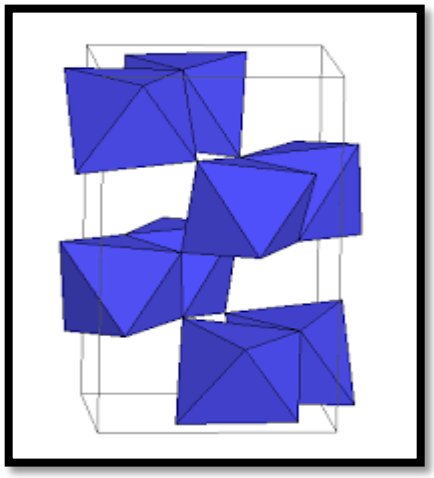

FIG 1.7, CRYSTAL STRUCTURE OF BROOKITE

1.12. HYDROTHERMAL METHOD:

The hydrothermal method has been widely used to synthesize TiO_2 nanocrystals. The TiO_2 nanocrystals are easily synthesized by carefully selecting the hydrthermal conditions such as temperature, reaction time and reactant concentration [32]. Hydrothermal processing can be defined as any heterogeneous reaction in the presence of aqueous solvents or mineralizers under high pressure and temperature conditions to dissolve and recrystallize (recover) materials that are relatively insoluble under ordinary conditions [33]. In comparison with sol-gel method [34-35], hydrothermal synthesis is an easy route to prepare a well-crystalline oxide under the moderate reaction condition, i.e. low temperature and short reaction time [36].

1.12.1. ADVANTAGES OF HYDROTHERMAL METHOD:

- Hydrothermal media provides an effective reaction environment for the synthesis of nanocrystalline TiO with high purity, good dispersion and well-controlled crystalline.
- The reactivity of a precursor system can be judged only by optimizing the processing variables such as starting materials, pH, and temperature [37].
- The hydrothermal synthesis in supercritical after has advantages for synthesis of multi metal oxide compounds because the reaction rate is enhanced more than 103 times that under the conventional hydrothermal conditions owing to the low dielectric constant as well as products with high crystallinity [38].

1.13. OBJECTIVES OF THE PRESENT WORK:

- Hydrothermal synthesis of TiO_2 nanoparticles.
- Conformation of Phase using Raman analysis.
- Structural characterization and Morphological study.
- I-V characterisation study.

REFERENCE:

1. R. Eisenberg and D.G. Nocera; overview of the forum on solar and renewable energy, Inorganic Chemistry: 44, 6799, 2005.
2. BP Statistical Review of World Energy; Bp London, 2010.
3. Americas Climate Choices; Panel on advancing the science of climate change, National research council: 2010.
4. Renewable Global Status Report; Renewable Energy Policy Network for the 21st Century: 2013.
5. M. Contreras, B. Egaas, K. Ramanathan, J. Hiltner, A. Swartzlander, F. Hasoon and R. Noufi, Prog. Photovolt: 7, 311, 1999.
6. N. S. Lewis, toward cost-effective solar energy use. Science: 315(5813), 798–801, 2007.
7. K, Honda and A. Fujishima Nature: 238, 37-39 1972.
8. B. O'Regan and M. Gratzel Nature: 353, 737-739 1991.
9. Michael Gratzel; Recent advances in sensitized mesoscopic solar cells: 42 (11), 1788-1798, 2009.
10. Andrea Listorti, Brian O'Rega and James R Durrant; Electron transfer dynamics in dye sensitized solar cell: 23 (15), 3381-3399, 2011.
11. X.F. Wang, J. Xiang, P. Wang and Y. Koyama ; Dye sensitized solar cells using chlorophyll a derivate as the sensitizer and carotenoids having different conjugation lengths as redox spacers, Science Direct: Chem. Phys. Lett: 408, 409-414, 2005.
12. M.A.Green, K.Emery, Y. Hishikawa, W. Warta, E.D. Dunlop; Solar Cell Efficiency Tables (Version 38), Progress in Photovoltics: 2011.
13. Sustainable Action Day, Desentizied Solar Cell: 2010.
14. S.S. Pradhan, S.K. Pradhan, V. Bhavanasi, S. Sahoo, S.N. Sarangi, S. Anwar, and P.K. Barhai; low temperature stabilized rutile phase TiO_2 films grown by sputtering, Thin Solid Films: 520, 1809-1813, 2011.

15. Moses Ezhil Raj, V. Agnes, V. Bena Jothy, and C. Sananjeeviraja; (Low temperature TiO_2 rutile phase thin film synthesis by chemical spray pyrolysis (CSP) of titanyl acetylacetonate, Mater. Sci. Semiconductor, Process: 13, 389-394, 2010.
16. V.N. Koparde and P.T. Cummings; phase transformations during Sintering of Titania Nanoparticles: 2, 1620-1624, 2008.
17. R.S. Rusu and G.I. Rusu; Journal of optoelectronics and advanced materials: 7, 234, 2005.
18. M. Nobial, O. Devos, and B. Tribollet; Advanced Techniques for Energy Sources, Investigations and Testing: 2011.
19. R. J. Gonzalez and R. Zallen, H. Berger; physics: 55, 7014, 1997.
20. M. Schuisky, A. Harsta, A. Aidla, K. Kukli, A. Keisler and J. Electrochem; 147, 3319, 2000.
21. Xiaobo Chen and Samuel S.Mao; Chem. Rev: 107, 2891, 2009.
22. P. J. Li, C. Ohtsuki, T. Kokubo, K. De Groot and J. Biomed; Material Science: 1994.
23. Y. Han, S. H. Hong and K. Xu; Mater. Lett: 56, 744, 2002.
24. C. Barret, and T. B. Massalki; Structure of Metals Clarendon Press, Oxford 1st edition: 1980.
25. Hanaor, and A.H. Dorian ; Sorrell, Charles C. (2011). "Review of the anatase to rutile phase transformation". Journal of Materials Science: 46 (4), 855–874, 2010.
26. M.H.Mangrola (Deapartment of Physics), V.N.S.G University, Surat: 2009.
27. Diebold and Ulrike; The surface science of titanium dioxide, Surface Science Reports: 48 (5-8): 53–229, 2003.
28. Y. Rong, Z. H. Chen, G. Wu, Wang and Mater; Chem. Phys: 91, 370, 2005.
29. S. Mahshid, M. Sasani Ghamsari, M.Askari, N.Afshar, and S.Lahuti, Semiconductor Physics, Quantum Electronics & Optoelectronics: 9, 65-68, 2006.
30. W. Zhou, Hong Liu, Robert I. Boughton, Guojun Du, Jianjian Lin, Jiyang Wanga and Duo Liua. J; Mater. Chem: 20, 5993-6008, 2010.
31. W.Hu, L.Li, G.Li, C.Tang, L.Sun; Hogh quality brookite TiO_2 flowers; Synthesis, characterization, and dielectric performance, Cryst. Growth Des: 9, 3676-3682, 2009X. Chen and S.S Mao; Chem. Rev: 107, 2891-2959, 2007.

32. K. Byrappa and M. Yoshimura; Handbook of Hydrothermal Technology, Noyes Publications: 2001.
33. J.Q. Huang, Z. Huang, W. Guo, Y.G. Cao and M.C. Hong; Cryst. Growth Des: 8, 2444, 2008.
34. H.W. Kim, H.S. Kim, H.G. Na, J.C.Yang. D.Y.Kim and J. Alloys Compd; 2010.
35. Y.V. Kolenko, A.A. Burukhin, B.R. Churagulov and N.N. Oleynikov, Mater. Lett: 57, 1124, 2003.
36. M.M. Lencka and R.E. Riman; Chem. Mater: 7, 18, 1995.
37. E. Chitanu and G. IOnita; hydrothermal growth of ZNO nanowires: 9-13, 2012.

REVIEW OF LITERATURE

CHAPTER II

REVIEW OF LITERATURE

2.1. INTRODUCTION:

This chapter deals with the literature review on synthesis of TiO_2 nanoparticles with different shapes were prepared by using different methods includes hydrothermal method, sol-gel method, microwave method and hydrothermal assisted methods and the characterization of the TiO_2 was carried.

Tran Trung *et al*., (2002) investigated the TiO_2 nanoparticles were prepared from titanium isopropoxide by using a new solvent system containing glycerol. The particle size of the sample was analyzed by scanning electron microscopy in the range of 4-10 nm. The X-ray diffraction data gives that the nanoparticle possesses a tetrahedral crystal structure of anatase phase. The UV spectra exhibited the tetrahedral titanium species at 280 nm of the quantum size effect of the nanoparticles [1].

Seigo Ito *et al*., (2007) investigated the fabrication of screen-printing pastes from TiO_2 powder for dye-synthesised solar cells. A preparation technique of TiO_2 screen-printing pastes from commercially-available powders has been disclosed in order to fabricate the nanocrystalline layers without cracking and peeling-off over 17 mm thickness for the photoactive electrodes of the dye-sensitized solar cells. A conversion efficiency of 87% was obtained by using a single-layer of a semi-transparent-TiO_2 film. A conversion efficiency of 92% was obtained by using double-layers composed of transparent and light-scattering TiO_2 films for a photon-trapping system [2].

Sorapong Pavasupree *et al*., (2007) synthesized Nanorods/nanoparticles TiO_2 with mesoporous structure by hydrothermal method at 150 °C for 20 h. The sample characterized by XRD, SEM, TEM, SAED, HRTEM, and BET surface area. The nanorods had diameter about 10-20 nm and the lengths of 100-200 nm, the nanoparticles had diameter about 5-10 nm. The prepared material had average pore diameter about 7-12 nm. The nanorods/nanoparticles TiO_2 with mesoporous structure showed higher photo

catalytic activity than the nanorods TiO_2, nanofibers TiO_2, mesoporous TiO_2, and commercial TiO_2 [3].

Daoai Wang *et al*., (2008) synthesized anatase TiO_2 nanotubes with the diameter of about 12 nm and the length of several hundred nanometers via hydrothermal method. The samples were characterized by X-ray diffraction (XRD), transmitting electron microscopy (TEM), X-ray photoelectron spectroscopy (XPS) and Brunauer Emmet Teller (BET) measurements. The nanotubes are used to make composites photoanode with pristine TiO_2 nanoparticles in dye-sensitized solar cells (DSSCs) and found that the NT/nanoparticle ratio had a pronounced impact on the performance of solar cells. [4].

Shrike *et al*., (2010) investigated the pure anatase TiO_2 nanoparticle were prepared by microwave assisted sol gel method and further characterization by powder. The SEM image gives the TiO_2 nanoparticles were porous structure. The XRD pattern indicated that the TiO_2 after annealed at 300°C for 3 hours forms purely anatase phase. The crystallite size was in the range of 20-25 nm from TEM image [5].

Liu min *et al*., (2010) reported that the three dimensional lower like anatase TiO_2 nanostructures and flower like titania nanostructures were successfully synthesized via hydrothermal synthesis followed by post treatment from titanium powder. The flower like anatase TiO_2 nanostructures was characterized in detail with SEM, XRD, UV-Vis spectrum measurement have a high specific surface area and a large light harvesting efficiency [6].

Chang hyo lee *et al*., (2011) synthesize TiO_2 nanotube by a hydrothermal method. The TiO_2 nanotube was coated on FTO glass by screen printing. The dye-sensitized solar cells were fabricated using ruthenium (II) (N719) dye and electrolyte. The crystalline structure and morphology were characterized by X-ray diffraction (XRD), and scanning electron microscopy (SEM). The absorption spectra were measured by UV-visible spectrometer. The diameter of the TiO_2 particles depends on the different hydrothermal temperatures [7].

Cong-hua Zhou *et al.*, (2011) synthesized TiO_2 sols via hydrothermal reaction using a less hydrolysable alkoxide or tetrabutyl titanate as the starting material. Using characterizations of X-ray diffraction, dynamic laser scattering and transmission electron microscopy, particle coarsening dynamics along with the particle dispersion behavior in the sols were studied via changing hydrothermal temperature from 160 °C to 250 °C and was observed that, pure anatase phase was obtained in the whole examined temperature range. With temperature increasing, the particle size distribution in the sols first narrowed, and then broadened. Mono-dispersed nanocrystallites were obtained at the temperature of 220 °C [8].

Tacchini *et al.*, (2011) Synthesized mono-dimensional titanium oxide nanostructures (multi-walled nanotubes and nanorods) by the hydrothermal method and applied to the construction of dye sensitized solar cells (DSCs). First, nanotubes (TiNTs) and nanotubes loaded with titanium oxide nanoparticles (TiNT/NPs) were synthesized with specific surface areas of 253 m^2/g and 304 m^2/g, respectively. After that, thermal treatment of the nanotubes at 500 °C resulted in their transformation into the corresponding anatase nanorods (TiNT and TiNT/NPs samples). X-ray diffraction and Raman spectroscopy data indicated that titanium oxide in the pristine TiNT and TiNT/NP samples was converted into anatase phase TiO_2 during the heating. Additionally, specific surface areas and water adsorption capacities decreased after the heat treatment due to the sample agglomeration and the collapse of the inner nanotube channels. DSCs were fabricated with the nanotube TiNT and TiNT/NP samples and with the anatase nanorod TiNT and TiNT/NPs samples as well. The highest power conversion efficiency of η = 3.12% was obtained for the TiNT sample, despite its lower specific surface compared with the corresponding nanoparticle-loaded sample (TiNT/NP) [9].

R. Vijayalakshmi *et al.*, (2012) compared TiO_2 nanoparticles prepared via two different routes; i) via sol-gel route and ii) by hydrothermal method and found that when prepared under the same ambient conditions temperature, pressure and keeping all the parameters same viz precursors, mole ratio, solvent etc; the nanoparticles prepared via sol-gel route were highly crystalline and had smaller crystallite size (~ 7 nm) as

compared to the one prepared by hydrothermal method (~ 17 nm). The crystallinity and the crystallite size were examined by XRD and TEM [10].

Geetha *et al.*, (2012) prepared TiO_2 nanoparticles using acid modified sol-gel method by varying different mole % of Chromium and characterized by various advanced techniques such as powder XRD, SEM, FESEM, UV-Vis, and photo voltage current. The results demonstrate that the pure TiO_2 and Cr-doped could inhibit the phase transformation, increase the surface area and decrease the crystallite size. UV-vis DRS spectrum revealed that the absorption was improved in both the ultra -violet and visible areas [11].

Qiaolin Han *et al.*, (2012) prepared nanocrystalline TiO_2 via hydrothermal synthesis using tetrabutyl titanate as starting material with a constant reaction time of 12 h at120 to 160°C and the pH value of the reaction medium was ranged from 1 to 9. Each specimen of the as-prepared TiO_2 powder was characterized by XRD, SEM, TEM, high-resolution transmission electron microscopy, selected area electron diffraction and was also used to fabricate dye sensitized solar cells (DSSCs). The result showed that the phase of the powder was affected by the pH value, whereas the particle size depended on the reaction temperature. Pure anatase TiO_2 was obtained with the pH value of 3. The solar energy conversion efficiency (η) of the DSSC fabricated with the pure anatase TiO_2 prepared at 140°C was 3.64%, which was higher than those with the TiO_2 prepared under any other conditions [12].

Geetha *et al.*, (2012) prepared TiO_2 nanoparticles by acid modified sol-gel method by varying different mole % of Chromium and characterized by various advanced techniques such as powder X-ray diffraction, SEM, FESEM, UV-vis, PL and photo voltage current. Analytical results demonstrated that the pure TiO2 and Cr-doped could inhibit the phase transformation, increase the surface area and decrease the crystallite size. UV-vis DRS spectrum revealed that the absorption was improved in both the ultra -violet and visible areas. Under simulated solar illumination, a short circuit current of 9.820 mA and an open circuit voltage of 0.714V were attained, which were better than the absorption of N719 dyes molecules with the photo anode materials [13].

Ming-Jer Jeng *et al*., (2013) prepared TiO_2 thin films from TiO_2 powders by using hydrothermal method and found that the synthesized TiO_2 nanorods were thin and long when smaller TiO_2 particles were used, while larger TiO_2 particles produced thicker and shorter nanorods. They also found that TiO_2 films prepared by TiO_2 nanorods exhibited larger surface roughness than those prepared by the commercial TiO_2 particles. The dye-sensitized solar cells fabricated with TiO_2 nanorods exhibited a higher solar efficiency than those fabricated with commercial TiO_2 nanoparticles directly [14].

Ming-Jer Jeng *et al*., (2013) synthesized nanocrystalline materials by hydrothermal method with high purity and well-controlled crystallinity. They used various sizes of commercial TiO_2 powders and used the hydrothermal method to prepare TiO_2 thin films. They found that the synthesized TiO_2 nanorods were thin and long when smaller TiO_2 particles were used, while larger TiO_2 particles produced thicker and shorter nanorods. They also found that TiO_2 films prepared by TiO_2 nanorods exhibited larger surface roughness than those prepared by the commercial TiO_2 particles. The dye-sensitized solar cells fabricated with TiO_2 nanorods exhibited a higher solar efficiency than those fabricated with commercial TiO_2 nanoparticles directly [15].

Bing-Xin Lei *et al*., (2014) prepared TiO_2 hollow spheres with outer diameter of 1.0-2.5 μm and shell thickness of 200 nm via a facile hydrothermal method without use of any template agent. The as-prepared TiO_2 hollow spheres are crystalline of the anatase phase, and possess a specific surface area of 48 $m^2 g^{-1}$. A high power conversion efficiency of 7.68% is achieved for dye-sensitized solar cell based on TiO_2 hollow sphere photo anode, representing a 16% efficiency boost over that of 6.65% achieved with the P25 based DSSC [16].

Govindaraj *et al*., (2014) prepared anatase phase TiO_2 nanostructures were prepared by two different methods and were characterized with Powder X-ray diffraction (PXRD), Field emission scanning electron microscopy (FESEM) and High resolution transmission electron microscopy(HRTEM) analysis. The PXRD pattern shows that both the nanostructures are anatase phase with good crystalline nature. The morphological results show that the TiO_2 nanorods have diameter of about 25 nm and the length of 100

nm. The TiO_2 nanoparticles are spherical in shape with mesoporous property. The solar energy conversion efficiency (η) of the cell using nanoparticles with mesoporous structure was about 3.415% with Jsc of 13.206mA/cm2, Voc of 0.607 V and FF of 43 %; while efficiency of the cell using nanorods reached 1.21% with Jsc of 4.35mA/cm2, Voc of 0.661V and FF of 42% [17].

Kyung Chul Sun *et al*., (2014) Studied different nanostructures of TiO_2 which play an important role in the kinetics of dye sensitized solar cells and affect the overall light harvesting efficiency of the cells. Pure anatase TiO_2 nanotubes were synthesized by a hydrothermal method using commercial material (P25) and to enhance the power conversion efficiency of the DSSC, a new type of double layered photoanode was prepared and optimized by using TiO_2 nanoparticles as the main layer and TiO_2 nanotubes by electrochemical measurement systems. The cells having the TNT over-layer showed longer electron life time, higher BET surface area and pore volume and 40% improved light harvesting efficiency [18].

Ari A.Mohammed *et al*., (2015) studied the fabrication of dye sensitized solar cell based on titanium dioxide by using two glass plates coated with Fluorine Tin Oxide. Titanium dioxide is applied to the conductive side of one plate and the other plate is coated with graphite. A dye is adsorbed on to the TiO_2 layer and then the plates are sandwiched together. A drop of iodide electrolyte is then added between the plates under a lamp emitting all wavelengths in the visible spectrum were not found to provide consistent data due to substantial heating of the cell. The outdoor tests carried out in natural sunlight exhibited steady voltage at much higher level [19].

Sasirekha *et al*., (2015) synthesized Titanium dioxide nanoparticles by chemical reduction route. The room temperature XRD pattern and micro-Raman spectra confirmed the formation of pure anatase TiO_2 nanoparticles. The Scanning electron micrograph revealed the formation of spherical shaped TiO_2 nanoparticles. The crystallite size was estimated as 16nm and 12nm using Phonon confinement model (PCM) and Debye Scherrer formula, respectively. The TiO_2 film was coated on ITO substrate by doctor blade technique and the film was sensitized with different natural dyes. The absorption

properties of the dyes and dye anchored TiO_2 films were analyzed by diffuse reflectance spectra (DRS) [20].

Lijian Meng *et al.*, (2015)., prepared TiO_2 nanorods by DC reactive magnetron sputtering technique and applied to dye-sensitized solar cells (DSSCs) and the length of the TiO_2 nanorods was varied from 1 μm to 6 μm. The scanning electron microscopy images show that the nanorods are perpendicular to the substrate. Both the X-ray diffraction patterns and Raman scattering results show that the nanorods have an anatase phase; no other phase has been observed. (101) and the (220) diffraction peaks have been observed for the TiO_2 nanorods and were used as the working electrodes in DSSCs and the effect of the nanorod length on the conversion efficiency of 4.8% has been achieved for 4 μm length nanorods [21].

Shi *et al.*, (2015) studied the effects of different hydrothermal synthesis conditions on the performance of dye-sensitized solar cells to improve photoelectric conversion efficiency. Nano-TiO_2 and doped nano-TiO_2 materials were prepared by hydrothermal synthesis method to making DSSC. Dye adsorption capacity and photo absorption characteristic were analyzed using ultraviolet and visible light(UV-vis)spectroscopy, Scanning electron microscope(SEM) was employed to observe surface morphologies of the TiO2 films and was concluded that nano-TiO_2 film electrodes that made by the hydrothermal synthesis method have larger special surface areas. The dye adsorption capacity of TiO_2 film under the condition of hydrothermal synthesis at 230℃/12 h is largest [22].

Mario *et al.*, (2015) synthesized anatase nanoparticles were from titanium isopropoxide solution using a hydrothermal process at different pressures in an autoclave system while keeping the volume of the solution constant. The crystal size of the nanoparticle increases as the autoclave pressure was increased. The anatase nanoparticles were used to build dye-sensitized solar cells (DSSC). Mesoporous films of this oxide were deposited over conducting SnO_2. The morphology of the mesoporous film surface of anatase was studied using scanning electron microscopy. The effects of the anatase synthesis conditions and properties of the mesoporous film on the DSSC-type solar cell

parameters, η%, V_{OC}, J_{SC}, and FF, were also investigated: the mesoporous anatase films prepared at 200 °C (54 atm of pressure in the autoclave) and annealed at 530 °C in air generated the best solar cell, having the highest conversion efficiency [23].

REFERENCE:

1. Tran Trung, Won-Jei Cho and Chang-Sik Ha; Material latters: 57, 2746-2750, 2003.
2. Seigo Ito, Peter Chen, Pascal Comte, Mohammad Khaja Nazeeruddin, Paul Liska, Pe´ter Pe´chy and Michael Gra¨tzely; Fabrication of Screen-Printing Pastes From TiO2 Powders for Dye-Sensitised Solar Cells: 4 (2), 1183-1190, 2012.
3. Sorapong Pavasupree, Supachai Ngamsinlapasathian, Yoshikazu Suzuki and Susumu Yoshikawa, Hydrothermal Synthesis of Nanorods/Nanoparticles TiO_2 for Photocatalytic Activity and Dye-sensitized Solar Cell Applications: 43, 149–157, 2008.
4. Daoai Wang, Bo Yu, Feng Zhou, Chengwei Wang and Weimin Liu: 2008.
5. B.S. Shrike, zhaung, H. Zhao and Y. Feng; nanotechnology: 18, 2010.
6. LIU min, Lu Wei-Ming, ZHAO lei, ZHOU chun-Ian, WANG Wen-jing and Trans; Nonferrous-Met.soc.china: 20, 2299-2302, 2010.
7. Chang hyo lee, Kyung uk jang, Hyung wook choi, Kyung hwan kim and Sang jun park; Synthesis of TiO_2 Nanotube by Hydrothermal Method and Application for Dye-Sensitized: 539, 125=[465]–132=[472], 2011.
8. Cong-hua Zhou, Sheng Xu, Ying Yang, Bing-chu Yang, Hao Hu, Zu-ci Quan, Bobby Sebo[b], Bo-lei Chen, Qi-dong Tai, Zhen-hua Sun and Xing-zhong Zhao, Titanium dioxide sols synthesized by hydrothermal methods using tetrabutyl titanate as starting material and the application in dye sensitized solar cells: 56, 4308-4314, 2011.
9. I. Tacchini, A. Ansón-Casaos, Youhai Yu, M.T. Martínez and M. Lira-Cantu; Hydrothermal synthesis of 1D TiO_2 nanostructures for dye sensitized solar cells: 177, 19-26, 2012.
10. R. Vijayalakshmi and V. Rajendran; Synthesis and characterization of nano-TiO2 via different methods: 4 (2), 1183-1190, 2012.

11. M. Geetha, K. Suguna and P. M. Anbarasan; Photoanode Modification in DSSC Using Chromium Doped TiO2 nanoparticles by sol-gel method: 3 (4), 303-308, 2012.
12. Qiaolin Han, Min Yu and Jiang Liu; Nanocrystalline titanium dioxide prepared by hydrothermal method and its application in dye-sensitised solar cells: 8(5), 238-242, 2013.
13. M. Geetha, K. Suguna and P. M. Anbarasan; Photoanode Modification in DSSC Using Chromium Doped TiO2 nanoparticles by sol-gel method: 3 (4), 303-308, 2012.
14. Ming-Jer Jeng, Yi-Lun Wung and Liann-Be; Chang and Lee Chow: 2013.
15. Ming-Jer Jeng, Yi-Lun Wung, Liann-Be Chang and Lee Chow; Dye-Sensitized Solar Cells with Anatase TiO2 Nanorods Prepared by Hydrothermal Method: 1-8, 2013.
16. Bing-Xin Lei, Ping Zhang, He-Kang Qiao and Xiao-Feng Zheng, : Yan-Shan Hu, Guo-Lei Huang, Wei Sun, Zhen-Fan Sun , Xian-Xi Zhang, A facile template-free route for synthesis of anatase TiO_2 hollow spheres for dye-sensitized solar cells: 3, 129–134, 2014.
17. R.Govindaraj, M. Senthil Pandian, P. Ramasamy1 and Sumita Mukhopadhyay; Synthesis of titanium dioxide nanostructures and their effects on current-voltage (I-V) performance in dye sensitized solar cells: 6, 5220-5225, 2014.
18. Kyung Chul Sun, Muhammad Bilal Qadir and Sung Hoon Jeong; Hydrothermal synthesis of TiO_2 nanotubes and their application as an over-layer for dye-sensitized solar cells: 4, 23223-23230, 2014.
19. Ari A. Mohammed, Alan S. Said Ahmad and Wafaa A. Azeez; Fabrication of Dye Sensitized Solar Cell Based on Titanium Dioxide: 2015.
20. P. Jayabal1, V. Sasirekha, J. Mayandi and V. Ramakrishnan; Synthesis and characterization of TiO2 nanoparticles for dye sensitized solar cell applications: 1, 01-10, 2015.
21. Lijian Meng, Hong Chen, Can Li and M.P. dos Santos; Preparation and characterization of dye-sensitized TiO_2 nanorod solar cells: 577, 103-108, 2015.

22. F. , C.Li, J. Li and X. Gao; Hydrothermal synthesis for thin film electrode of dye-sensitized solar cells and its performance: 31(3), 507-515, 2015.
23. Mario Alberto Sánchez-García, Xim Bokhimi, Arturo Maldonado-Álvarez, and Antonio Esteban Jiménez-González; Effect of Anatase Synthesis on the Performance of Dye-Sensitized Solar Cells: 10, 306, 2015.

METHODOLOGY AND METHODS

CHAPTER III

METHODOLOGY AND METHODS

3.1. INTRODUCTION:

This chapter describes the experimental techniques used in the preparation and characterization of pure anatase TiO_2 nanoparticles using hydrothermal synthesis method. The TiO_2 nanoparticles were characterized using X-ray diffraction (XRD), Scanning Electron Microscope (SEM), Raman spectroscopy and UV-Visible analysis in order to identify the crystal size and morphology, crystal phase and the absorbance in the UV-Visible region of TiO_2.

3.2. HYDROTHERMAL SYNTHESIS METHOD:

The method is based on the ability of water and aqueous solutions to dilute at high temperature (500°C) and pressure (10-80 MPa) substances practically insoluble under normal conditions: some oxides, silicates, sulphides. The main parameters of hydrothermal synthesis, which define both the processes kinetics and the properties of resulting products, the duration and temperature of synthesis, and the pressure in the system. The synthesis is carried out in autoclaves which are sealed steel cylinders that can withstand high temperatures and pressure for a long time [1].

3.3. CHEMICALS AND GLASSWEARS USED:

- Titanium isopropoxide (97% pure)
- Autoclave
- Magnetic stirrer and pellets
- Muffle furnace

3.4. METHOD OF ANNEALING:

Annealing is a method of heat treatment that alters the physical and chemical properties of a material to increase its ductility and reduce its hardness, making it more workable. It involves heating a material to above its recrystallization temperature, maintaining a suitable temperature, and then cooling. In annealing, atoms migrate in the crystal lattice and the number of dislocations decreases, leading to the change in ductility and hardness [2].

3.4.1. STAGES OF ANNEALING:

There are three stages of annealing process which are preceded as the temperature of the material is increased. The three stages are

- Thermal recovery
- Recrystallization
- Grain growth

The thermal recovery is the cold work properties begin to disappear. Slight decreases in tensile strength and no change in ductility and all the residual stress is reduced. The Recrystallization is a strained grain becomes stress free, strain free grains. Microstructure at the end of recrystallization is much similar to the original structure prior to the cold working. The temperature at which the normal cold worked material recrystallizes in one hour. It temperature is high in case of metal having high melting point. Then grain growth stage is the grain size and number of the recrystallized structure depends on the amount of prior cold working. On repeated annealing larger grains consume smaller grains. At the end of annealing the number of grain decreases and the size increases.

3.5. METHOD OF PREPARATION:

3.5.1. PREPARATION OF PURE TiO_2:

The synthesis of anatase TiO_2 nanoparticles by hydrothermal method was carried out using the reagents Titanium isopropoxide (TI (IV) IP, 97% pure) and Glycerol (99% pure). The solution was taken under the volume ratio of 1:25. In this method Titanium isopropoxide was added drop by drop with Glycerol under continuous stirring using the magnetic stirrer at room temperature. The solution was stirred for several minutes to get a homogeneous solution. The solution was placed in a stainless steel autoclave for subsequent hydrothermal reaction for 13 hours at 180°C. The autoclave was cooled down to room temperature in which the solution turns the white precipitate. This white precipitate was left for aging up to several hours after which the solution was heated and dried to get TiO_2 powder which is shown in fig 3.1. The TiO_2 nanopowder was kept for annealing at temperature of 450°C in the muffle furnace. The constant 450°C was maintained and after which the annealed powder was allowed to cool at room temperature.

SCHEMATIC REPRESENTATION FOR EXPERIMENTAL PROCEDURE

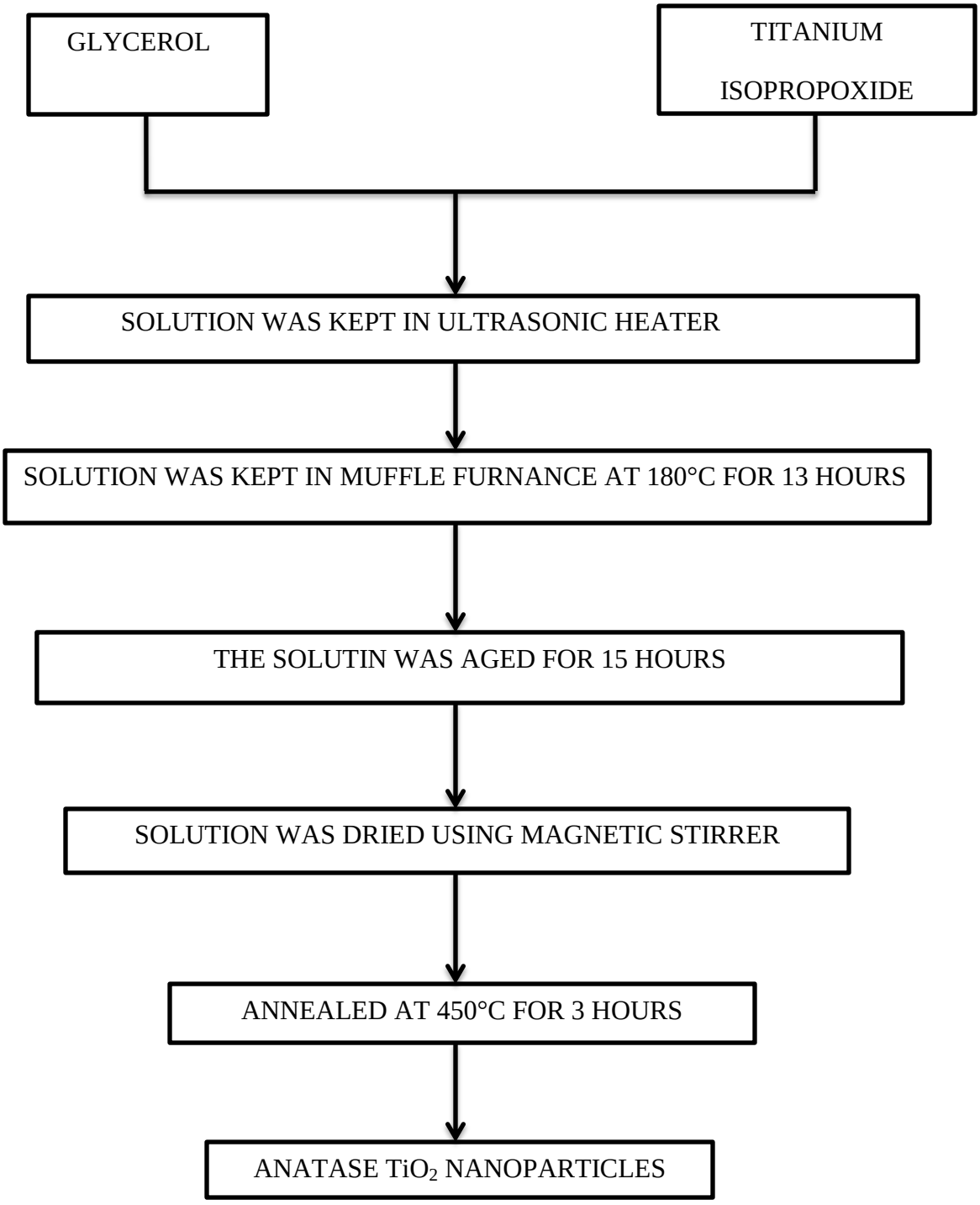

FIG 3.1, SYNTHESISED TITANIUM DIOXIDE POEDER USING HYDROTHERMALMETHOD

3.6. PREPARATION FOR ANODE:

3.6.1. PASTE PREPARATION:

- The TiO_2 nano powder was taken.
- The sample was transferred it into an Agate mortar.
- Mixed with required amount of Ethanol for several minutes.
- Paste was prepared.

3.6.2. SUBSTRATE CLEAN:

The Fluorine doped tin-oxide (FTO) conducting substrates was ultrasonically cleaned with soap solution, ethanol, acetone and distilled water for 10 min each and finally the substrates are dried in air.

3.6.3. ANODE PREPARATION:

- Conducting surface of FTO was identified.
- Small amount of TiO_2 paste was taken and spread it uniformly over the FTO substrate with glass rod.
- The TiO_2 coated substrates were heated to remove the organic solvents.
- Crack free was confirmed.

3.6.4. DYE PREPARATION:

0.03 mM concentration of N719 dye was prepared with ethylene glycol.

The dye solution is always needed to be stored away from light. The TiO_2 film was immersed in the N719 dye solution. It was kept overnight at room temperature to absorb the dye on the TiO_2 surface.

3.6.5. PREPARATION OF COUNTER ELECTRODE:

The glass substrates consist of conducting layer which acts as a counter electrode. For efficient regeneration of the redox couple, a layer of platinum is often coated on the substrate. Alternatively there is also another counter electrode such as carbon black and polymers are used. In this work carbon is used as a counter electrode.

The counter electrode was prepared with the pencil which leaves a dark shade of carbon on the FTO glass.

3.6.6. ELECTROLYTIC SOLUTION:

Iodine and potassium Iodide has been chosen for making electrolyte solution.

- Using the electronic balance, the exact amount of chosen compound was measured.
- The measured compound was mixed with Ethylene glycol and stirred. It is ensured that the entire compound has been completely dissolved.
- This solution was used as an electrolytic solution

3.7. STRUCTURAL AND MORPHOLOGICAL STUDIES:

3.7.1. X – RAY DIFFRACTION (XRD):

When a beam of X rays is incident on an atomic plane making an angle θ and leaves the atomic plane so as to produce the diffraction pattern. The phenomenon is called X-Ray diffraction. XRD is a rapid analytical technique primarily used for phase identification of crystalline material and can provide information on unit cell dimensions. XRD is a very important experimental technique that has been used for long time to study the crystal structure of solids, lattice constants and geometry, orientation of single crystals, defects, stresses etc [3].

3.7.2. X-RAY POWDER DIFFRACTION METHOD:

Powder XRD is perhaps the most widely used x-ray diffraction technique for characterizing materials. As the name suggests, the sample is usually in a powdery form, consisting of fine grains of single crystalline material to be studied. The technique is used widely for studying particles in liquid suspensions or polycrystalline solids.

The term 'powder' really means that the crystalline domains are randomly oriented in the sample. Therefore when the 2-D diffraction pattern is recorded, it shows concentric rings of scattering peaks corresponding to the various d spacing in the crystal lattice. The positions and the intensities of the peaks are used for identifying the underlying structure (or phase) of the material. For example, the diffraction lines of graphite would be different from diamond even though they both are made up of carbon atoms. This phase

identification is important because the material properties are highly dependent on structure.

Powder diffraction data can be collected using either transmission or reflection geometry, as shown below. Because the particles in the powder sample are randomly oriented, these two methods will yield the same data [4].

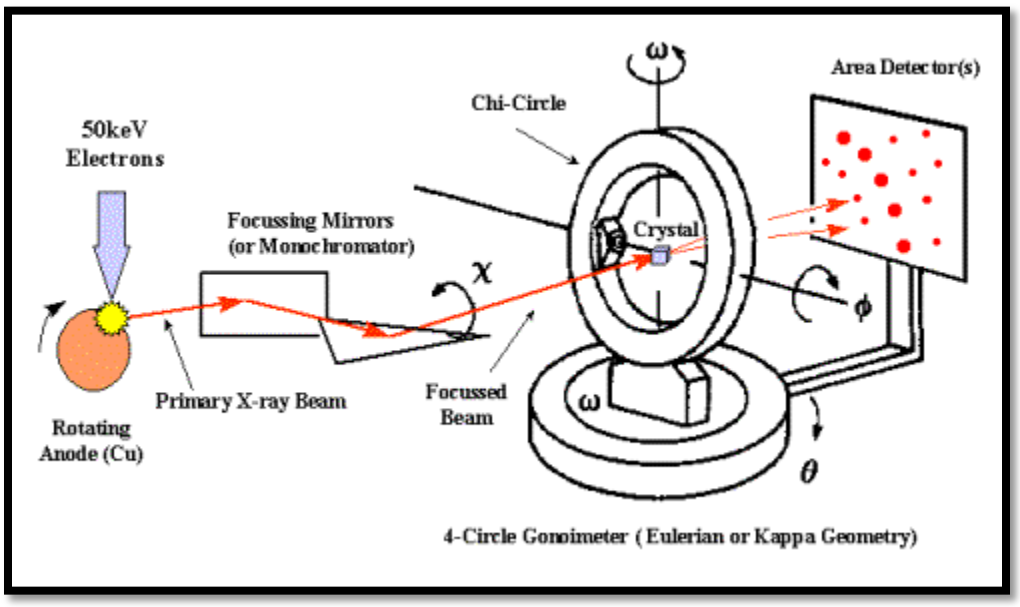

FIG 3.2, SCHEMATIC REPRESENTATION OF WORKING OF XRD

3.7.3. Bragg's Formula:

The structures of crystals and molecules are often being identified using x-ray diffraction studies, which are explained by Bragg's Law. The law explains the relationship between an x-ray light shooting into and its reflection off from crystal surface.

$$n\lambda = 2d\sin\theta$$

Where

• n is an integer,
• λ is the wavelength of x-rays, and moving electrons, protons and neutrons,
• d is the spacing between the planes in the atomic lattice, and
• θ is the angle between the incident ray and the scattering plane [5].

The intensity of the diffracted X-ray is measured as a function of the diffraction angle 2θ and the specimen orientation. This law relates the wavelength of electromagnetic radiation to the diffraction angle and the lattice spacing in a crystalline sample. These diffracted X-rays are then detected.

3.7.4. Scherrer equation:

Based on the XRD pattern of the sample the crystalline size was calculated using the Debye scherrer's formula is given by,

$$D = K \lambda / \beta \cos\theta$$

K is the Scherrer's constant of the order of unity,

λ is the X-ray wavelength,

β is the full width of height maximum (FWHM) of a diffraction peak,

Θ is the diffraction angle [6].

3.8. FIELD EMISSION SCANNING ELECTRON MICROSCOPE:

3.8.1. DEFINITION:

The FESEM is a microscope that works with electron instead of light. These electrons are liberated by a field emission source. The object is scanned by electrons in a zigzag pattern.

A FESEM is used to visualize very small topographic details on the surface or entire or fractioned objects.

3.8.2. INSTRUMENTATION:

VACUUM:

The FESEM can be classified as a high vacuum instrument (less than 1x10-7 Pa in the gun zone). The vacuum allows the electron movement along the column without scattering and it helps to prevent the discharge inside the gun zone.

FIELD EMISSION SOURCE:

The function of the electron gun is to provide a large and stable current in a small beam. There are two classes of emission source: thermionic emitter and field emitter. Emitter type is the main difference between the Scanning Electron Microscope (SEM) and the Field Emission Scanning Electron Microscope (FESEM). Thermionic Emitters use electrical current to heat up a filament; the two most common materials used for filaments are Tungsten (W) and Lanthanum Hexaboride. When the heat is enough to overcome the work function of the filament material, the electrons can escape from the material itself. Thermionic sources have relative low brightness, evaporation of cathode material and thermal drift during operation. Field Emission is one way of generating electrons that avoids these problems. A Field Emission Gun (FEG); also called a cold cathode field emitter, does not heat the filament. The emission is reached by placing the filament in a huge electrical potential gradient. The FEG is usually a wire of Tungsten fashioned into a sharp point. The significance of the small tip radius (~ 100 nm) is that an electric field can be concentrated to an extreme level, becoming so big that the work

function of the material is lowered and electrons can leave the cathode. FESEM uses Field Emission Gun producing a cleaner image, less electrostatic distortions and spatial resolution < 2nm.

ANODES:

The FESEM has two anodes for electrostatic focusing. A voltage (0 ~ 5 KV) between the field emission tip and the first anode, called the extraction voltage, controls the current emission (1 ~ 20 micro-A). A voltage (1 ~ 30KV), called the accelerating voltage, between the cathode and the second anode increases the beam energy and determines the velocity at which the electrons move into the column. This voltage combined with the beam diameter determines the resolution (capacity to resolves two closely spaced point as two separates entities). As voltage increases, better point to point resolution can be reached.

ELECTRO MAGNETI LENSES:

To resolve a feature on the specimen surface, the beam diameter must be smaller than the feature (still containing high current density). Therefore it is necessary to condense the electron beam. To assist in the demagnification of the beam, electromagnetic lenses are employed. A lower level of the beam condensation is necessary to have a probe useful for image processing. This makes the FESEM the highest resolution instrument.

APERTURE:

Variable apertures are used to refine the beam. Small objective aperture sizes will produce better resolution, good depth of field and minimal charging. It is the responsibility of the user to choose the correct aperture size.

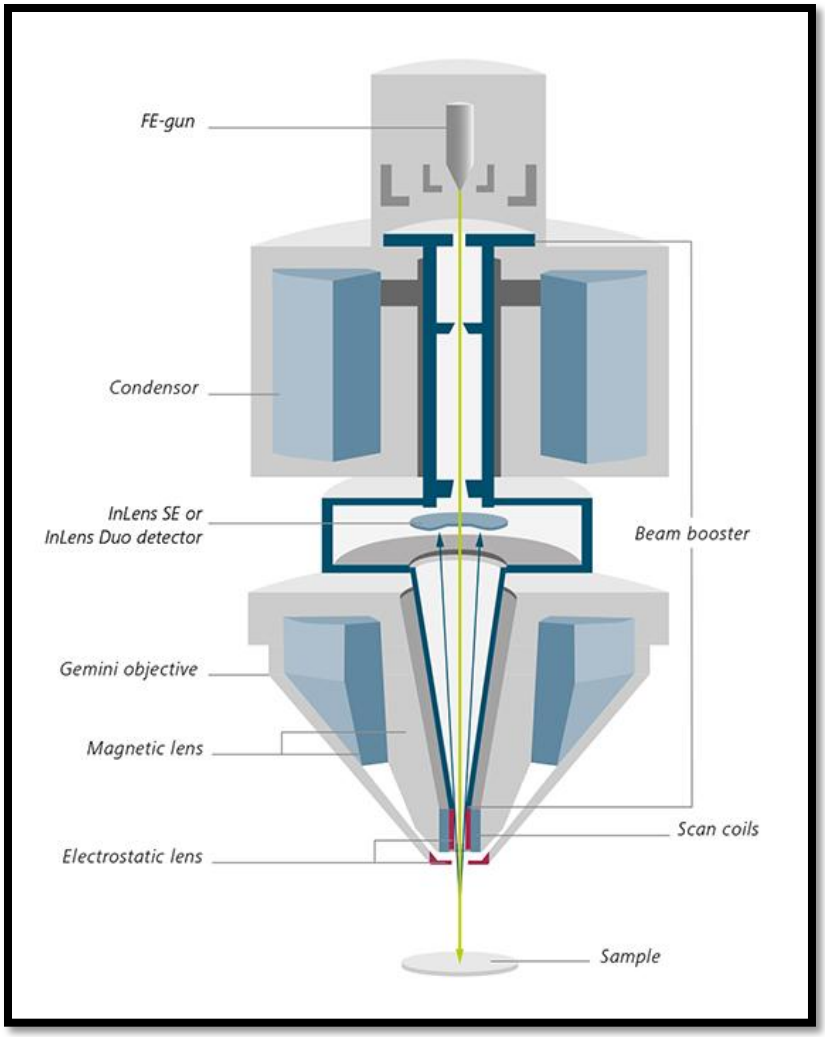

FIG3.3, SCHEMATIC REPRESENTATION OF WORKING OF FESEM

DEPTH OF FIELD:

Depth of Field is important in routine microscopy and represents the ability to maintain the focus even with large changes in specimen topography. Long working distance (the distance from the final objective lens to the specimen surface) and small aperture yields images that appear in focus over a large change in Z-axis.

ELECTRON BEAM AND SPECIMEN INTERACTION:

The specimen and the electron beam interact in both elastic and inelastic fashion giving different types of signals. Elastic scattering events are those that do not affect the kinetic energy of the electron even when its trajectory had been affected. Inelastic scattering events are a result of the energy transfer from the electron beam to the atoms in the specimen. As a result the electrons have energy loss with small trajectory deviation. Each of these signals gets specific information about topography, crystallography, surface characteristics and specimen composition.

3.9. OPTICAL STUDIES:

3.9.1. RAMAN SPECTROSCOPY:

3.9.2. INTRODUCTION:

The Raman spectroscopy is a molecular spectroscopy which is observed as in elastically scattered light, allows for the interrogation and identification of vibrational (phonon) states of molecules. As a result, Raman spectroscopy provides an invaluable analytical tool for molecular finger printing as well as monitoring changes in molecular bond structure (e.g. state changes and stresses & strains).

3.9.3. INSTRUMENTATION:

The Raman spectroscopy is essentially an emission spectroscopy. The main components of a Raman spectrometer are,

- Radiation source
- Filters
- Sample tube
- Spectrograph

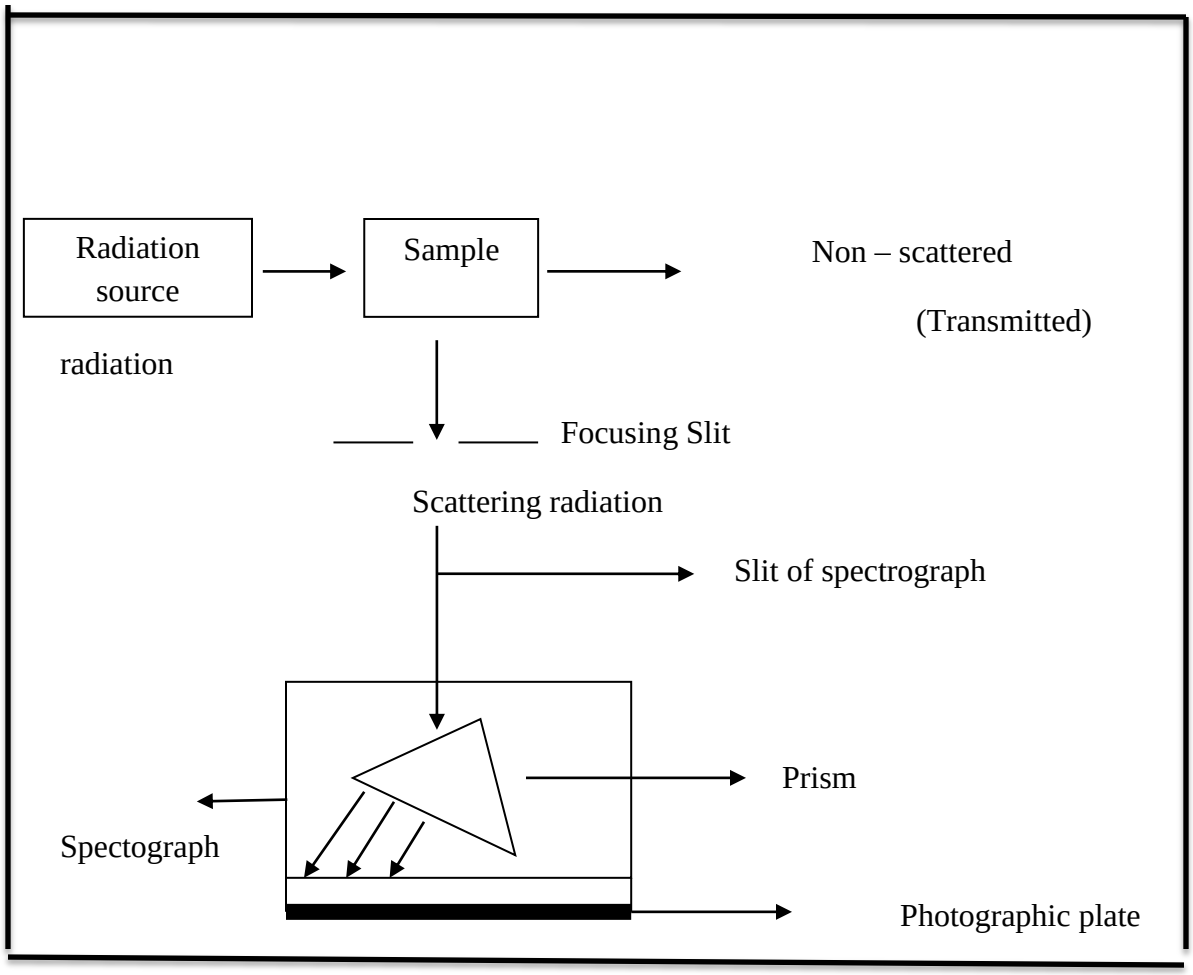

FIG 3.4, SCHEMATIC DIAGRAM OF RAMAN SPECTROMETER

RADIATION SOURCE:

Radiation source is essential to use a radiation of high intensity. The intensity of Raman lines is proportional to the fourth power of the frequency of incident radiation. Thus the excitation frequency which is high enough, but not so much as to cause photo decomposition of the sample is used. The mercury arc lamp is the most useful source of radiation. The most commonly used radiation in Raman spectroscopy is the line corresponding to 4358 Å which is obtained from the mercury arc lamp by use of suitable

filters. The laser is almost an ideal source of radiation for Raman spectroscopy and it is largely displacing the traditional mercury lamp. Helium-neon laser source has become very common, laser beam 6328 Å wavelength is generally employed. An argon-neon laser with lines at 4880 and 5145 Å are used, especially when higher intensity of Raman lines is required.

FILTERS:

The filter is the non-monochromatic incident radiation there will be overlapping of Raman shifts making the interpretation of the spectrum difficult. The monochromatic incident radiations are necessary. Filters are used to obtain monochromatic radiation. They are generally made of nickel oxide or quartz. Sometimes used a coloured solution.

SAMPLE TUBE:

The sample tube shape and size of the tube depends on the intensity of incident radiation, nature of the sample and its available amount. For gases relatively bigger tubes are required. Various types of sample tubes are in use for Raman spectroscopy.

SPECTROGRAPH:

The spectroscopy used in Raman spectroscopy should have large gathering power, hence, special prisms of high resolving power and short focus camera are used. A lens directs the scattered radiation upon the slit of the spectrograph and Raman lines can be obtained on a photographic plate. Raman spectrographs with automatic records are also available. However, due to low intensity of Raman lines, photographic method is preferred because it is more sensitive.

The intensity of Raman lines mainly depends on the polarizability of the molecules, intensity of the exiting radiation and concentration of Raman active species. The Raman intensities are directly proportional to the concentration of Raman active species [7].

3.10. CHARACTERISTICS OF I-V CURVE:

A current-voltage (I-V) curve is the possible combinations of current and voltage output of a photovoltaic (PV) device. The I-V characteristic curve which is short for Current-Voltage Characteristic Curves or simply I-V curves of an electrical device or component are a set of graphical curves which are used to define its operation within an electrical circuit. As its name suggests, I-V characteristic curves show the relationship between the current flowing through an electronic device and the applied voltage across its terminals.

3.10.1. SHORT CIRCUIT CURRENT:

The short-circuit current is the current through the solar cell when the voltage across the solar cell is zero (i.e., when the solar cell is short circuited). The short-circuit current is due to the generation and collection of light-generated carriers. For an ideal solar cell at most moderate resistive loss mechanisms, the short-circuit current and the light-generated current are identical. Therefore, the short-circuit current is the largest current which may be drawn from the solar cell.

The short-circuit current depends upon the solar cell area, the number of photons, the spectrum of the incident light, the optical properties, the collection probability.

3.10.2. OPEN CIRCUIT VOLTAGE:

The open-circuit voltage (V_{OC}) is the maximum voltage available from a solar cell, and this occurs at zero current. The open-circuit voltage corresponds to the amount of forward bias on the solar cell due to the bias of the solar cell junction with the light-generated current.

3.10.3. FILL FACTOR:

The short-circuit current and the open-circuit voltage are the maximum current and voltage respectively from a solar cell. However, at both of these operating points, the

power from the solar cell is zero. The FF is defined as the ratio of the maximum power from the solar cell to the product of V_{oc} and I_{sc}.

$$FF = \frac{I_{\max} X V_{max}}{I_{sc} X V_{OC}}$$

3.10.4. EFFICIENCY:

Efficiency is defined as the ratio of energy output from the solar cell to input energy from the sun. In addition to reflecting the performance of the solar cell itself, the efficiency depends on the spectrum and intensity of the incident sunlight and the temperature of the solar cell. Therefore, conditions under which efficiency is measured must be carefully controlled in order to compare the performance of one device to another.

$$\eta = \frac{I_{sc} X V_{oc} X FF}{P_{in}}$$

REFERENCE:

1. R. Churagulov, Lomonosov Moscow State University. Shlyakhtin Oleg A.Zaitsev Dmitry D, Churagulov Bulat R:
2. Van Vlack, L. H; Elements of Materials Science and Engineering. Addison-Wesley: 134, 1985.
3. T. Theivasanthi and M. Alagar; X-Ray Diffraction Studies of Copper Nanopowder.
4. B.E. Warren, General Publishing Company, 1969, 1990 (Classic x-ray physics book)
5. Bragg, W.L. The Crystalline State: Volume I. New York: The Macmillan Company, 1934.
6. L.S. Brisks and H. Friedman; Journal of Applied Physics; 17, 687, 1946.
7. L.D.S. Yadav, Organic spectroscopy: 107-121, 2013.
8. Youngmi Kim, Sujung Kim, Keepyung Nahm, and Misook Kang; Dynamic Rapid Synthesis of Bisnitrato Zinc (II) Nitrate Using a Microwave Method and its Application to Dye-Sensitized Solar Cells (DSSC); Bull. Korean Chem: 31, 2923, 2010.

RESULTS AND DISCUSSION

CHAPTER IV

RESULTS AND DISCUSSION

4.1. INTRODUCTION:

This chapter deals with the result of synthesized TiO_2 nanoparticles. The TiO_2 nanoparticles were prepared by hydrothermal method. The optical and structural study of the above sample was discussed by using X-Ray Diffraction, Field Emission Scanning Electron Microscope, Raman analysis and I-V characteristics.

4.2. STRUCTURAL CHARACTERISATION:

4.2.1. X-RAY DIFFRACTION ANALYSIS:

The prepared TiO_2 nanoparticles were investigated using X-Ray diffraction which is used to determine the characterization of crystalline structure materials. The diffraction pattern of the prepared sample (TiO_2) is shown in Fig 4.1.

The sharp diffraction peaks indicates that the obtained TiO_2 nanoparticles have high crystallinity and the full width half maximum of the peak conforms the existence of nanosize in the prepared sample. The peaks in 25.3621°, 37.8328°, 48.0717°, 54.0410°, 55.1435°, 62.7795°, 68.9210°, 70.3042°, 75.0776° are corresponding of the (hkl) miller indices values as (101), (004), (200), (105), (211), (204), (116), (220), (215) respectively. The peaks corresponding to the other two forms of TiO_2 namely rutile and brookite were not found. So that the above corresponding peaks have conformed the pure phase of the sample. The X-Ray diffraction pattern has good agreement with JCPDS card no: 894921 [1-2]. Moreover it corresponds to the anatase phase.

4.2.2. CRYSTALLITE SIZE CALCULATION:

The crystallite size of the TiO_2 nanoparticles can be determined from the corresponding X-Ray spectral peaks from Scherrer's formula, Eqn 1.

$$\mathbf{D} = \frac{K\lambda}{\beta \cos\theta} \longrightarrow (1)$$

$\lambda \longrightarrow$ is the wavelength of X-Ray diffraction (λ=0.15406 nm)

K $\longrightarrow$ is the Scherrer's constant (K=0.89) and

$\beta \longrightarrow$ is the line width at the half maximum height

$\theta \longrightarrow$ is the diffraction angle.

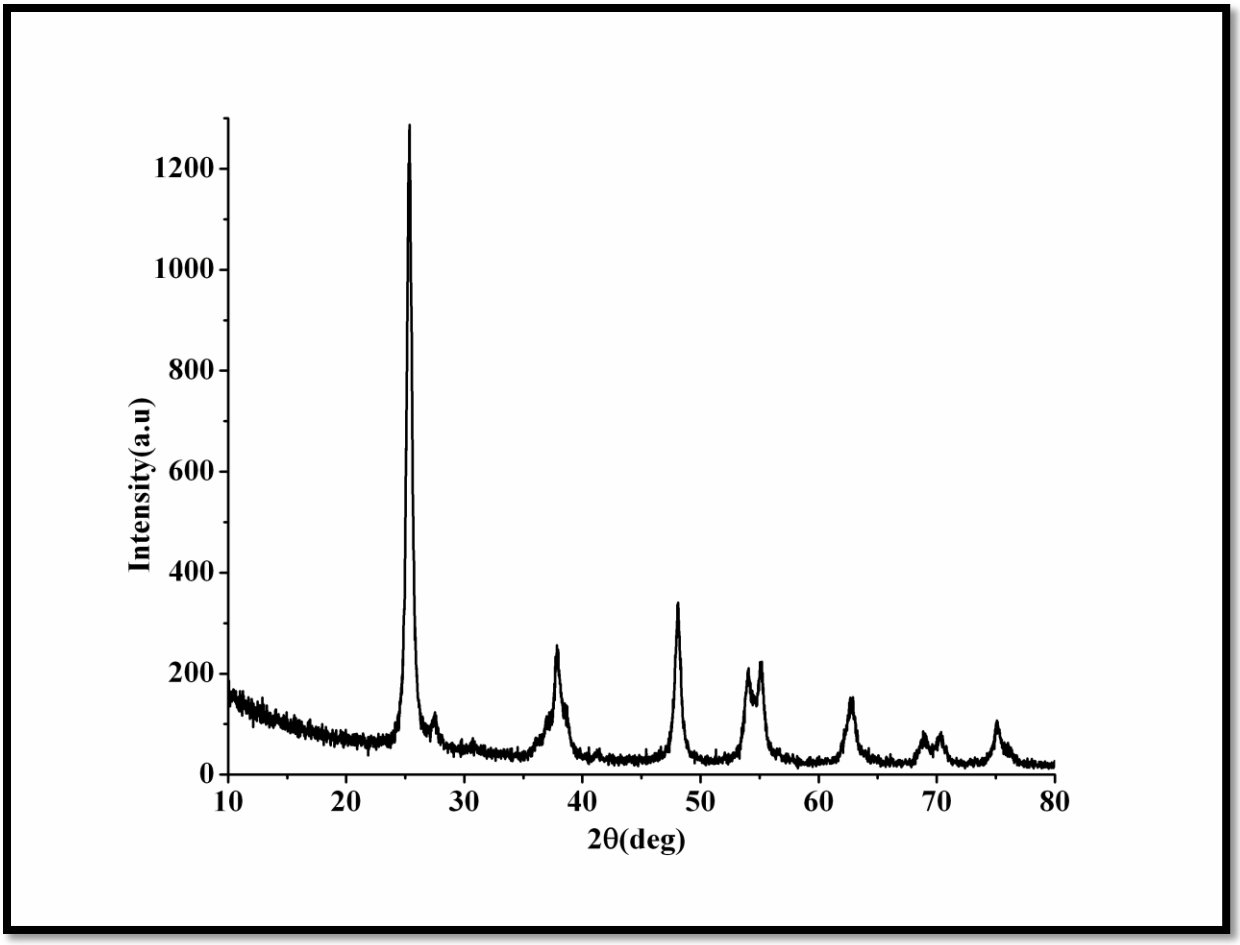

FIG 4.1, XRD SPECTRUM OF SYNTHESISED TiO_2 NANAOPARTICLES

The average crystallite size obtained from XRD data for pure TiO_2 nanoparticle is 21 nm which was calculated using Scherrer's formula. The crystallite size of prepared sample TiO_2 depends upon the preparation method and annealing temperature.

TABLE 4.1, COMPUTED VALUES OF CRYSTALLITE SIZE FOR TiO_2

2θ (deg)	FWHM (deg)	D=kλ/βcosθ (nm)	h	k	l
25.3621	0.3011	26.39	1	0	1
37.8328	0.3346	22.97	0	0	4
48.0717	0.2007	39.49	2	0	0
54.0410	0.4015	19.79	1	0	5
55.1435	0.4015	19.79	2	1	1
62.7795	0.3346	23.75	2	0	4
68.9210	0.6691	11.87	1	1	6
70.3042	0.5353	14.84	2	2	0
75.0776	0.5353	14.84	2	1	5

The above table (4.1) shows 2θ values are observed from the XRD pattern of TiO_2, FWHM values represent the Full Width Half Maximum from the XRD pattern and D(nm) values represent the crystallite size that calculated from the XRD pattern, miller indices (hkl) values are taken from reference JCPDS card no: 894921.

4.3. OPTICAL CHARACTERISATION:

4.3.1 RAMAN ANALYSIS:

Optical Raman Spectroscopy is a powerful tool to study the vibrational modes of TiO_2 and phase conformation of Titania samples. It can be used to identify the phases of TiO_2.

The Raman Spectrum of obtained TiO_2 nanoparticles in the region of 100 cm^{-1} to 700^{-1} is shown in fig 4.2. A well resolved Raman peaks were observed at 145 cm^{-1}, 194 cm^{-1}, 398 cm^{-1}, 514 cm^{-1} and 638 cm^{-1}. The obtained intensity distribution and the peak position are confirming the presence of the pure anatase phase only. There is no possibility for the existence of mixture of anatase and rutile phase or pure rutile phase. So it confirms the presence of pure anatase phase. The vibrational modes of Raman spectrum at 145cm^{-1} represents the symmetric stretching vibration of O-Ti-O, 398 cm^{-1} represents the symmetric bending vibration of O-Ti-O and 514 cm^{-1} represents anti-symmetric bending vibration of O-Ti-O. The Raman spectrum of anatase TiO_2 nanoparticles was obtained for the annealed sample. For annealing process 425°C was maintained about 3 hours. Table 3 shows the comparison of Raman peaks of prepared TiO_2 nanoparticles with the existing report [3-4].

TABLE 4.2, COMPARISON OF RAMAN PEAKS

TiO_2 NANOPARTICLE PREPARED	**NANOPARTICLE TiO_2 (REF 2).**
145 cm^{-1}	144 cm^{-1}
194 cm^{-1}	197 cm^{-1}
398 cm^{-1}	399 cm^{-1}
514 cm^{-1}	513 cm^{-1}
638 cm^{-1}	639 cm^{-1}

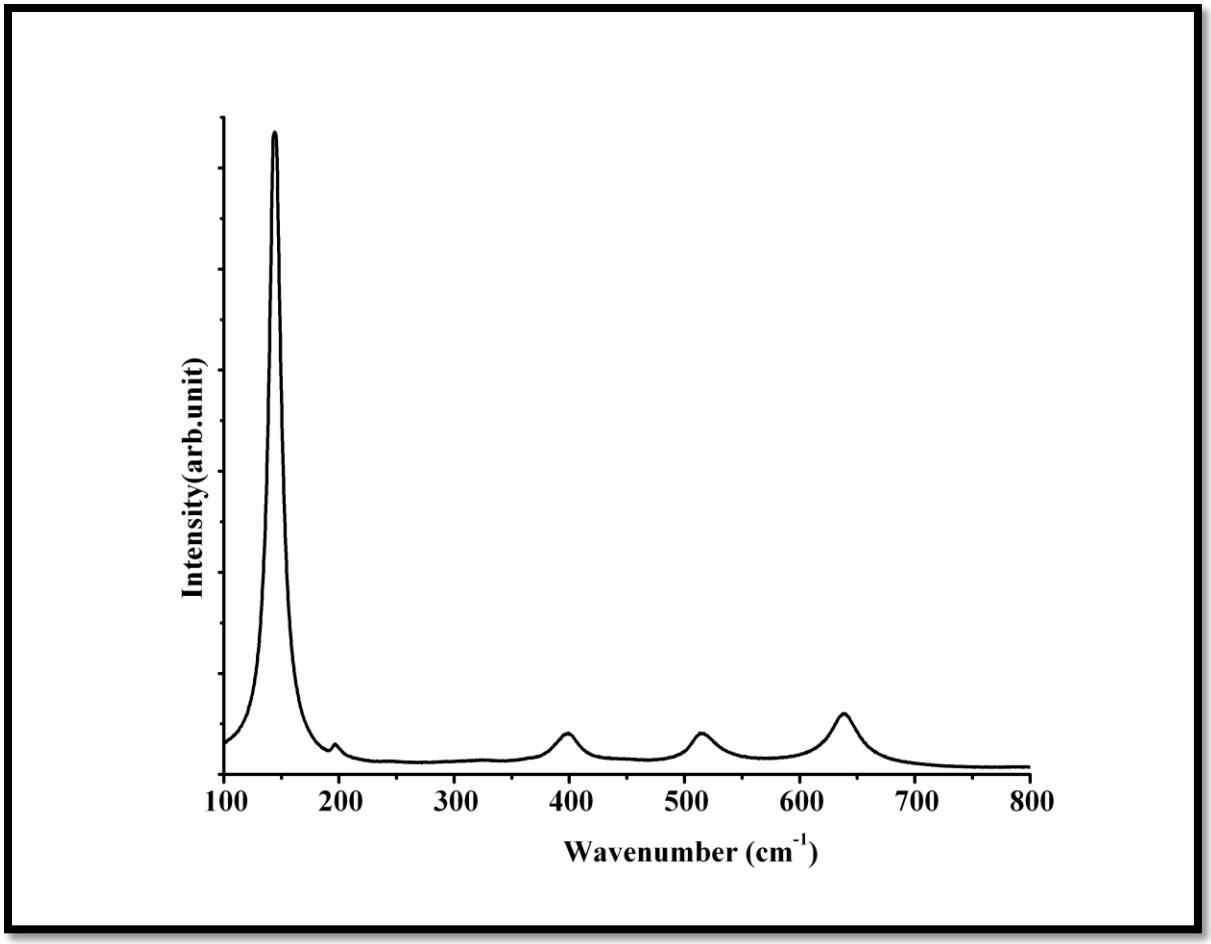

FIG 4.2, RAMAN SPECTRUM OF SYNTHESIZED TiO_2 NANOPARTICLES

4.4. MORPHOLOGICAL ANALYSIS:

4.4.1. FIELD EMISSION SCANNING ELECTRON MICROSCOPY ANALYSIS:

Field Emission Scanning Electron Microscope was used to characterize the external surfaces of the nanoparticles. For the morphological characterization, the anatase nano crystalline TiO_2 were characterized by FESEM. The FESEM images of TiO_2 nanoparticles are shown in figure 4.3, 4.4 and 4.5.

The temperature of hydrothermal process was 180°C for different hydrothermal times. The time duration for hydro thermal process were maintained for 13, 24 and 48 hours respectively [5].

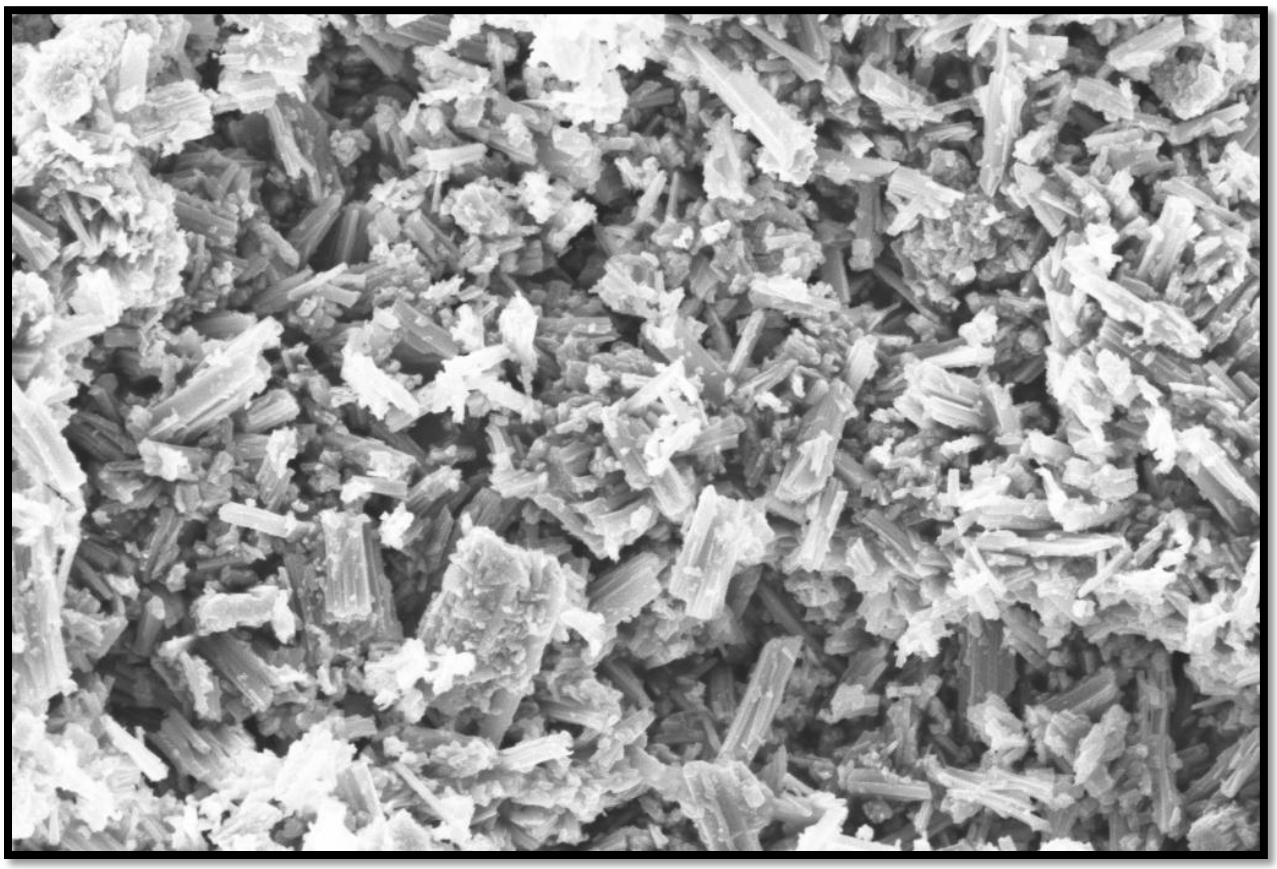

FIG 4.3, FESEM IMAGES OF SAMPLE SYNTHESIZED AT 180°C FOR 13 HOURS

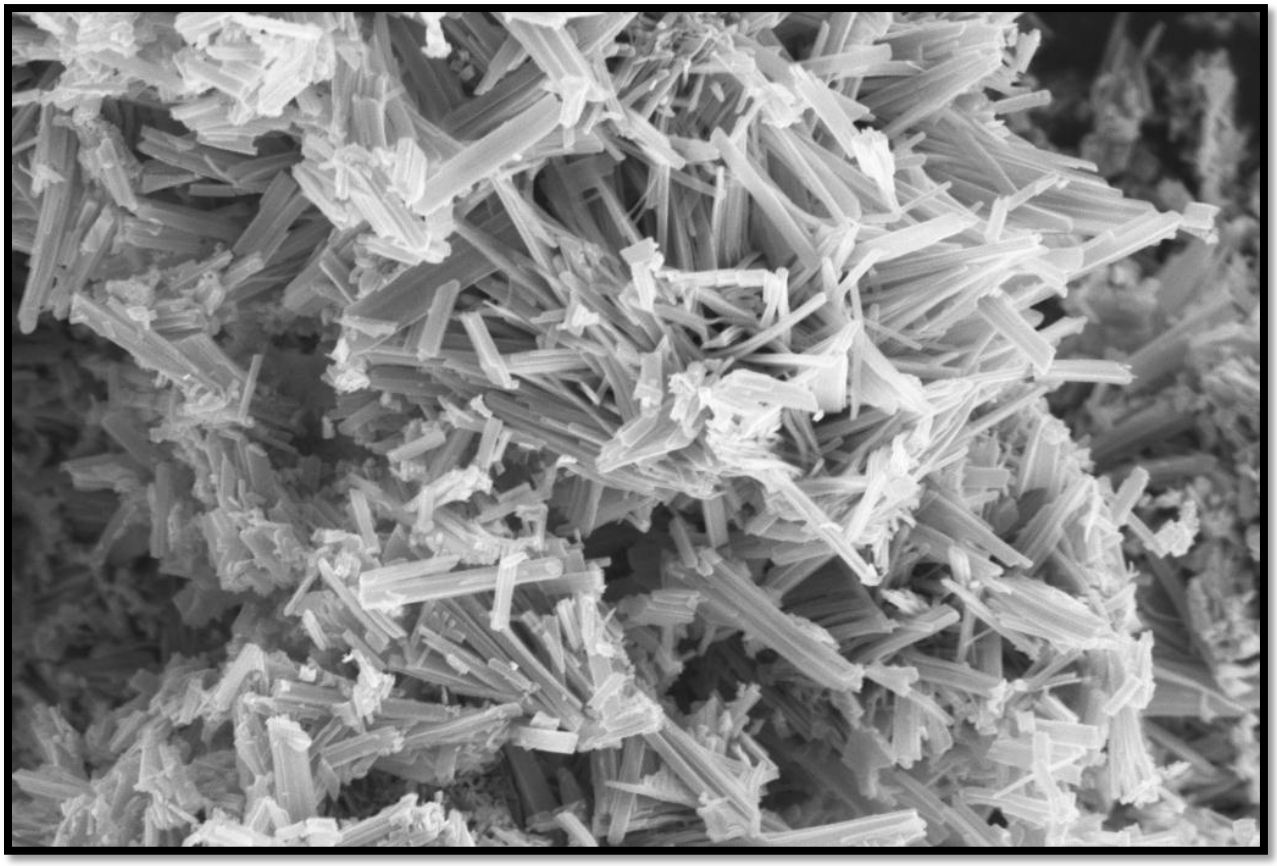

FIG 4.4, FESEM IMAGES OF SAMPLE SYNTHESIZED AT 180°C FOR 24 HOURS

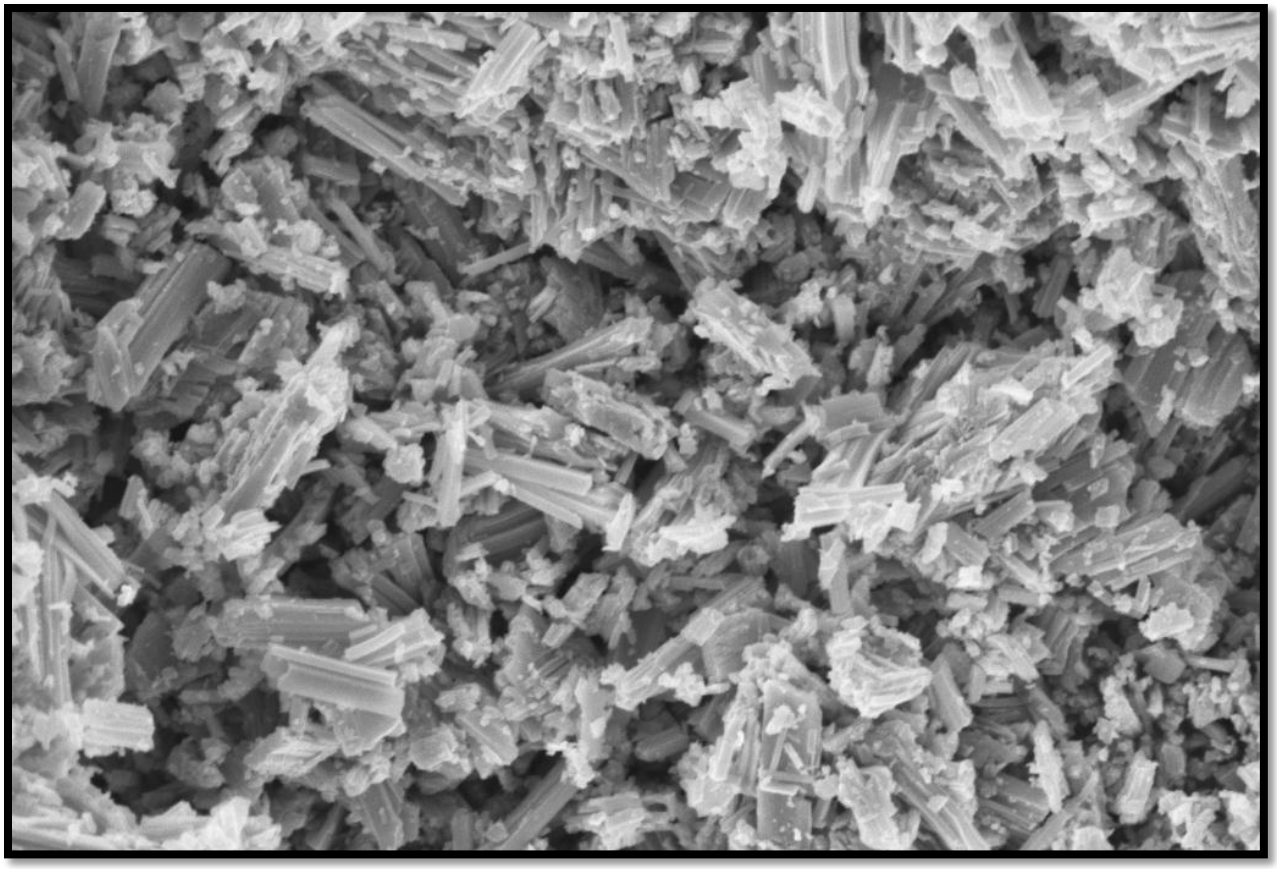

FIG 4.5, FESEM IMAGES OF SAMPLE SYNTHESIZED AT 180°C FOR 48 HOURS

The synthesized TiO_2 samples have been taken under the magnification of 30.00 KX which are shown in Figs 4.3, 4.4 and 4.5. The FESEM image evidenced the shape of the particle was not uniform and it looks like nanorods in shape. The formed nanorods are visible clearly. The TiO_2 nanoparticles were grown into different sizes.

TABLE 4.3, AVERAGE LENGTH AND BREADTH OF THE PREPARED SAMPLE

SAMPLE IN HOURS	LENGTH	BREADTH
13 hrs	900 nm	250 nm
24 hrs	1350 nm	150 nm
48 hrs	975 nm	100 nm

The length and breadth of the prepared samples are shown in table 4.3. However, increasing the time duration during synthesis leads to well dispersed nanorods with reduction of agglomeration. For 24 and 48 hrs it is observed that the particle possess clear nanorods in shape. Samples with very low aggregation can help to enhance the electrical properties of the material by improving the kinetics of electron which leads to improved electrical conductivity [6-7].

4.5. ELECTRICAL CHARACTERISATION:

4.5.1. I-V CHARACTERISATION:

Current voltage measurement is one of the most essential measurements of a solar cell. The I-V characteristics was measured by applying an external potential between the working and counter electrode.

The maximum power value (P_{max}) is 0.00016 Watts. Corresponding to this P_{max}, current maximum (I_{max}) and voltage maximum (V_{max}) were determined that is 0.760 mA and 0.211 V. From the I-V curve, short circuit current (I_{sc}) and open circuit voltages (V_o) values are obtained as 1.05 mA and 0.555 V respectively. The cell attained an efficiency of 0.641 (%) with fill factor (FF) of 0.275.

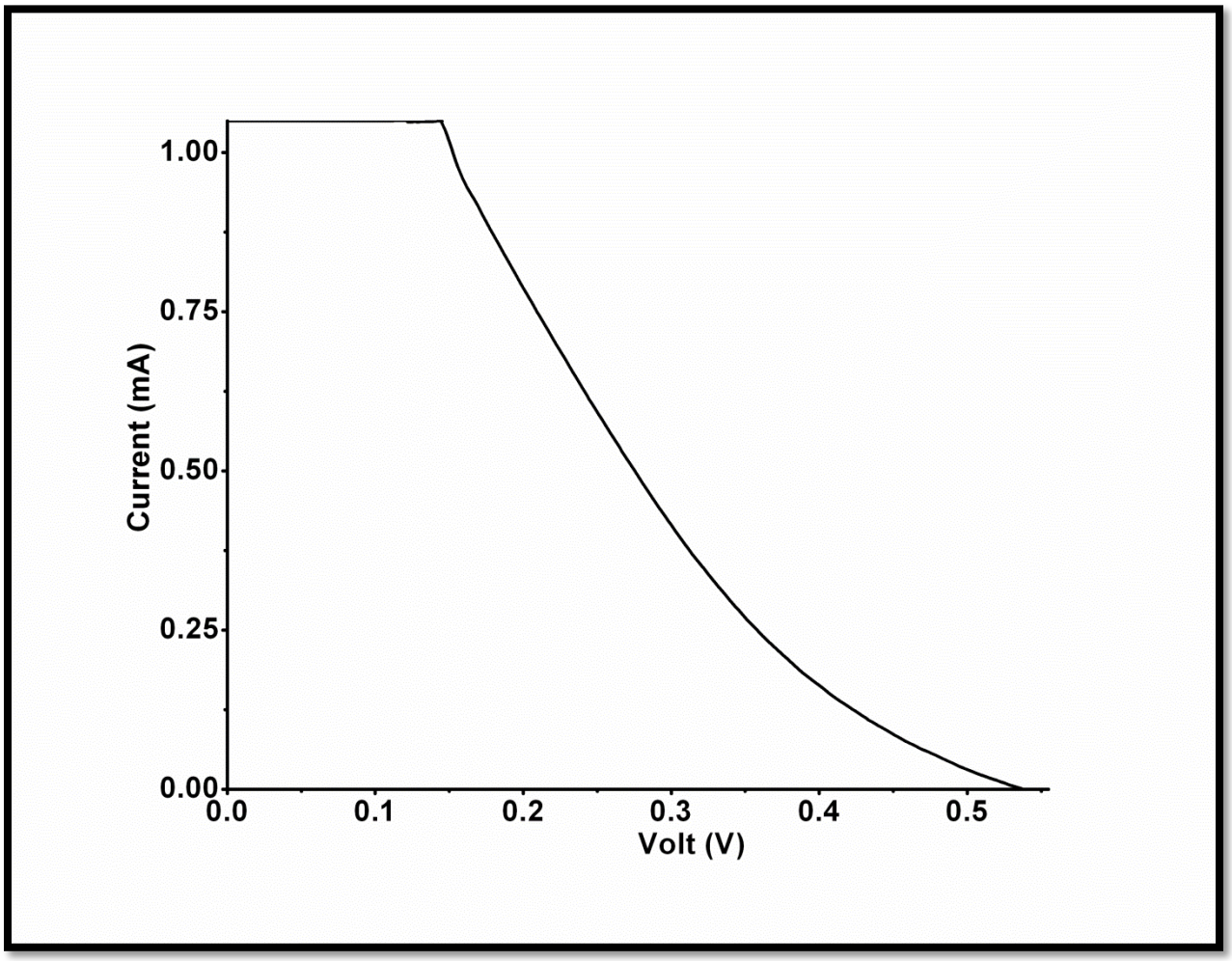

FIG 4.6, I-V CHARACTERISATION OF TiO_2 NANOPARTICLE

REFERENCE:

1. R.Vijayalakshmi, V.Rajendran; Arch.of.Appli. sci.Reas. : 4(2), 2014, 1183-1190.
2. Yue Kun Laia, Jian-Ying Huang, Hui-Fang Zhang, Vishnu priyaSubramaniam, Yu Xin Tang, Dang Guo Gong, LathaSundar, Lan Sun, Zhong Chen and Chang JIan Lin; Journal of Hazardous Materials, 184 (1-3), 2010, 855-863.
3. Suresh c. pillai, pradeepan periyat, reenamole george, declan e. McCormack, Michel K.Seery, hugh Hayden, John Colreavy, David Corr3 and Steven Hinder; Journal of physics Chemistry C:111, 4, 2007, 1605.
4. J. Preudhomme, P. Tarte, Spectrochim. Acta 28A, 69, 1972.
5. L. Yang, S. Luo, Q. Cai, and S. Yao: 55, 331 (2010).

SUMMARY AND CONCLUSION

CHAPTER V

SUMMARY AND CONCLUSION

Dye-sensitized solar cells (DSSC) are an efficient type of thin film photovoltaic cell. In the dye – sensitized solar cell, the semiconductor oxide materials are used for charge separation and charge transport. The basic element of DSSC is a nanostructured material. In the present research work, pure Anatase TiO_2 nanoparticles have been synthesized using hydrothermal method. The synthesized anatase TiO_2 nanoparticles have been subjected for different characterization techniques such as X-ray diffraction, Raman analysis, I-V characteristics and Field Emission Scanning Electron Microscope. The following conclusion can be summarized from the results obtained during this study,

- The crystalline size of anatase TiO_2 nanoparticles is 21 nm, calculated using X-ray diffraction analysis.
- The crystal structure of anatase TiO_2 nanoparticle is Tetragonal.
- The sharp diffraction peak of the sample indicates the high crystallinity and full width half maxima of the peak confirm the existence of nanosize.
- Raman spectrum demonstrates that the obtained nanopowder was well crystallized in the anatase phase.
- The vibrational modes of TiO_2 possess the Symmetric stretching, Symmetric bending and Anti-symmetric vibrations.
- The rods shape of anatase TiO_2 nanoparticle was confirmed from the Field Emission Scanning Electron Microscope at 180°C for 13, 24 and 48 hours.
- The average length and breadth of the TiO_2 nanoparticle is 900 nm and 250 nm for 13 hours, 1350 nm and 150 nm for 24 hours and 975 nm and 100 nm for 48 hours respectively.
- The overall maximum conversion efficiency was about 0.641 % from I-V measurement.